



Review

# Research Progress and Challenges of Carbon/MXene Composites for Supercapacitors

Li Sun <sup>1</sup>, Yu Dong <sup>1</sup>, Hangyu Li <sup>1</sup>, Hanqi Meng <sup>1</sup>, Jianfei Liu <sup>1</sup>, Qigao Cao <sup>1</sup> and Chunxu Pan <sup>2,\*</sup>

<sup>1</sup> Northwest Institute for Non-Ferrous Metal Research, Xi'an 710016, China

<sup>2</sup> MOE Key Laboratory of Artificial Micro- and Nanostructures, School of Physics and Technology, Wuhan University, Wuhan 430072, China

\* Correspondence: cxpan@whu.edu.cn

**Abstract:** Carbon materials/MXenes composite materials have gained widespread attention in the field of supercapacitors due to their excellent electrochemical performance. Carbon materials are considered ideal electrode materials for supercapacitors due to their high specific surface area, good conductivity, and outstanding electrochemical stability. MXenes, as a novel two-dimensional material, exhibit prominent conductivity, mechanical properties, and ionic conductivity, thereby showing great potential for applications in energy storage devices. The combination of carbon materials and MXenes is expected to fully leverage the advantages of both, optimizing electrode conductivity, enhancing the energy density and power density, and improving the charge–discharge performance. This article reviews the key research progress of carbon/MXenes composite materials in supercapacitors in recent years, including their synthesis methods, structural tuning, and improvements in their electrochemical performance. Finally, the article looks forward to future research directions and proposes potential strategies to enhance the overall performance of the composite materials and achieve large-scale applications. By addressing the existing challenges, carbon/MXenes composite materials are anticipated to achieve higher energy and power outputs for the supercapacitor field in the future, providing strong support for the development of new energy storage technologies such as electric vehicles and wearable devices.



**Citation:** Sun, L.; Dong, Y.; Li, H.; Meng, H.; Liu, J.; Cao, Q.; Pan, C. Research Progress and Challenges of Carbon/MXene Composites for Supercapacitors. *Batteries* **2024**, *10*, 395. <https://doi.org/10.3390/batteries10110395>

Academic Editors: Leon L. Shaw and Ottorino Veneri

Received: 29 September 2024

Revised: 28 October 2024

Accepted: 5 November 2024

Published: 7 November 2024



**Copyright:** © 2024 by the authors. Licensee MDPI, Basel, Switzerland. This article is an open access article distributed under the terms and conditions of the Creative Commons Attribution (CC BY) license (<https://creativecommons.org/licenses/by/4.0/>).

## 1. Introduction

With the rapid development of the global economy and the rapid advancement of technology, the utilization and storage technology of renewable energy has become an important research field [1–4]. Faced with the increasingly severe energy crisis and environmental pollution, it is particularly urgent to develop efficient energy storage devices. Researchers have conducted numerous studies into the development of sustainable and clean energy conversion and storage systems, such as supercapacitors, fuel cells, and metal ion batteries [5–8]. Supercapacitors, as a new type of energy storage device, are excellent electrochemical devices for energy storage in devices with high-quality energy batteries [8,9]. Supercapacitors have the advantages of fast charge–discharge, a long cycle life, and high power density, and are widely used in fields such as electric vehicles, renewable energy storage, large-scale power regulation, and other fields [2,10–12].

According to the charge storage mechanism, supercapacitors can be divided into double-layer capacitors and Faradaic-type capacitors [12–15]. Double-layer capacitors typically have a high power density due to the physical store of charges at the electrode–electrolyte interface through electrostatic attraction [2]. Carbon materials with a high specific surface area, excellent electronic conductivity, and stability are typical electrode materials for double-layer capacitors [16–18]. However, the low-mass density of carbon-based

electrode materials can lead to a lower energy density and volumetric capacitance of double-layer capacitors [19]. Faradaic-type capacitors store charges through rapid oxidation-reduction reactions, and have a high energy density but low cycling stability and rate performance, such as transition metal oxides/carbides and conductive polymers [17,20–22]. In view of this, scientists have conducted extensive research in an attempt to solve the dilemma faced by supercapacitors by developing novel electrode materials, including (1) enhancing the energy density and holding a high power density, (2) increasing the cycle stability to extend the service life, and (3) decreasing the expense and complexity of electrode materials [23–25].

MXenes, with a layered structure similar to graphene, are a novel two-dimensional (2D) material [26,27]. Since the first report in 2011, the distinctive properties and structure of MXenes have led to their widespread research in the field of energy storage and conversion [28]. MXenes are constructed alternately with carbon layers and transition metal layers, exhibiting outstanding conductivity ( $Ti_3C_2T_x$  up to  $10,000\text{ S cm}^{-1}$ ) and a rapid electron transfer [29]. In addition, due to the highly ion accessibility of the 2D layered structure and functionalized surface, MXenes can provide double-layer capacitance, intercalation pseudocapacitance, and redox pseudocapacitance [30]. Due to the magnitude of the electrostatic potential difference at the electrode–electrolyte interface and the types of electrolyte ions and surface terminations, the charge storage mechanism in MXene is a non-singular and interchangeable process [1,2,24]. MXenes may exhibit a double-layer capacitance mechanism in environments lacking  $H^+$ , such as  $K_2SO_4$  and KOH electrolytes. However, the charge storage is mainly dominated by pseudocapacitive behavior in acidic electrolytes (such as 3 M  $H_2SO_4$  electrolyte) [6,19]. The  $H^+$  ions undergo highly reversible protonation/deprotonation at the -O terminal of MXenes in the electrolyte [6,10]. In the neutral and alkaline electrolytes, the electrolyte ions act as a dielectric medium to prevent the hybrid orbital between the ions and the MXenes surface terminal, forming a double electric layer [6,10]. On the contrary, MXenes exhibit the combination of double-layer capacitance, intercalation pseudocapacitance, and REDOX pseudocapacitance due to the polarization voltage and the surface terminal composition in the acidic electrolyte [15]. When MXenes are heavily modified by other functional groups, the double-layer capacitance dominates due to the protonation reaction triggered only by the -O terminal [6,23]. When a sufficient negative voltage is applied, the adsorption potential of the intercalated positive ions can be overcome, and hybrid orbitals allow hydrogen ions to directly adsorb with single-bond O terminals, generating intercalation pseudocapacitance [6,28]. As the negative potential increases, the single-bond O terminal continuously adsorbs ions and converts into a single-bond -OH terminal, expanding the MXenes intermediate layer under electrostatic repulsion [6]. As the interlayer space continues to expand, more and more MXenes surfaces are exposed, and ions undergo rapid surface redox reactions, producing redox pseudocapacitance [10]. Modified MXenes have more ion transport channels, which will reduce ion diffusion resistance and improve the electrochemical performance [31]. However, there are strong van der Waals interactions and hydrogen bonding between the MXene nanosheets, which can easily lead to re-stacking and self-oxidation in practical applications, resulting in a decrease in the accessible surface area and a decline in the capacitance performance [32,33]. Secondly, MXenes, such as  $Ti_3C_2T_x$ , undergo a reaction when in contact with air or moisture. Non-conductive  $TiO_2$  will form due to the oxidation of surface Ti atoms through the interaction of oxygen or  $H_2O$ , which reduces electronic conductivity and capacitance active sites, leading to a deterioration in the electrochemical performance [18]. In addition, MXenes-based supercapacitor devices face challenges such as severe self-discharge behavior and limited potential windows.

To overcome the above problems, researchers have found that introducing conductive spacers with stable structures (such as molybdenum carbide, carbon materials, polymers, metal oxides, etc.) into the intermediate layer of MXene nanosheets is an effective and feasible strategy [34–36]. The phenomenon of MXene nanosheets restacking and aggregation can be suppressed, and consecutive electron transport channels and extra capacity can also

be provided. Carbon materials have an ultra-high specific surface area, excellent electrical conductivity, good chemical stability, and an outstanding electrochemical performance [37]. Carbon materials are mainly based on adsorbing ions to construct double-layer capacitors for energy storage. Therefore, the contact area between the electrode and the electrolyte is increased by increasing the specific surface area, so as to raise the double-electric-layer capacitance [37]. With the maturity and expansion of functionalization technology for carbon materials, carbon materials with a Faradaic-type capacitors mechanism have attracted widespread attention from researchers, especially heteroatom-doped carbon materials. The difference in electronegativity between heteroatoms and carbon atoms will modify the electronic structure, promote electron migration, increase the surface activity of the material, and thus improve the electrochemical performance [37]. The introduction of heteroatoms into carbon materials can transfer high electrochemical active sites and change the reactivity and kinetics of the material through unconventional charge polarization [37]. Moreover, the abundant active sites enable Faraday reactions to store more charges, significantly improving the specific capacitance and energy density. Moreover, carbon materials with various nanostructures can be introduced into the MXenes structure to prevent re-stacking, including zero-dimensional (0D) (carbon quantum dots (CQDs), carbon spheres), one-dimensional (1D) (carbon nanotubes (CNT), carbon nanofibers (CNF)), 2D (graphene nanosheets, carbon nanosheets), three-dimensional (3D) (graphene foam, activated carbon) [17,19,23,25]. In addition, carbon materials not only protect MXenes from oxidation to a certain extent, but also reduce the oxidation reaction rate of MXene [17]. Carbon materials coating the surface of MXenes can inhibit oxidation reactions, as oxidants such as oxygen and water are isolated [19]. The introduction of MXenes into carbon materials can increase the interlayer spacing of nanosheets, thus overcoming the structural defects of MXenes [23]. The electron transfer ability and electrochemical performance of carbon/MXenes can be effectively improved through the synergistic effect of carbon materials and MXenes [25]. In recent years, some researchers have confirmed and summarized that the application of carbon/MXene composite materials in supercapacitors has a significant impact on improving the electrochemical performance. Therefore, the introduction of two-dimensional MXenes into carbon materials to construct and improve the microstructure to fully exploit the electrochemical properties has become a widely sought after solution. Zhang et al. summarized the emerging technologies of MXenes and carbon hybridization, and their applications in lithium storage, sodium storage, lithium sulfur batteries, supercapacitors, and electrocatalysis [18]. However, the new preparation strategies of carbon-MXene composites (such as 3D printing technology) and the effects of the introduction of carbon with different structures into MXenes on the performance of supercapacitors require a more in-depth and detailed summary. Cai et al. introduced the definition of MXenes, common strategies for synthesizing  $Ti_3C_2T_x$ , and the latest progress of  $Ti_3C_2T_x$ /carbon composite materials as electrode materials for supercapacitors [23]. Nevertheless, further discussion is needed on the preparation strategy and system classification of carbon MXene composite materials, as well as the influence of the existing states of carbon materials with different structures on the performance of supercapacitors. Siddhu N. K. et al. briefly reviewed the structure, surface termination, and synthesis of MXenes and MXene/carbon composite materials, as well as their applications in the field of supercapacitors [17]. Further review is needed on the preparation strategies and clear classification of carbon MXene composite materials. Although the above article provides a review of the application of carbon/MXene composite materials in the field of supercapacitors, with the continuous research and exploration of new preparation technologies and construction strategies, the systematic classification and in-depth analysis of preparation techniques and the introduction of carbon materials with different structures into MXenes to achieve their full performance still have important significance.

This article comprehensively summarizes the research progress of traditional and emerging carbon materials/MXenes composites in the field of supercapacitors. Furthermore, we have reclassified and summarized the synthesis methods of carbon/MXene

composites and focused on discussing the role of different structured carbon materials in regulating the structure/properties of MXenes and improving the electrochemical performance, as shown in Figure 1, as well as how to achieve the effect of “1 + 1 > 2”. Classifying carbon/MXene composites based on their carbon size and analyzing the main challenges and future research directions of carbon/MXene composites as electrode materials for supercapacitors can provide useful guidance for researchers in related fields.

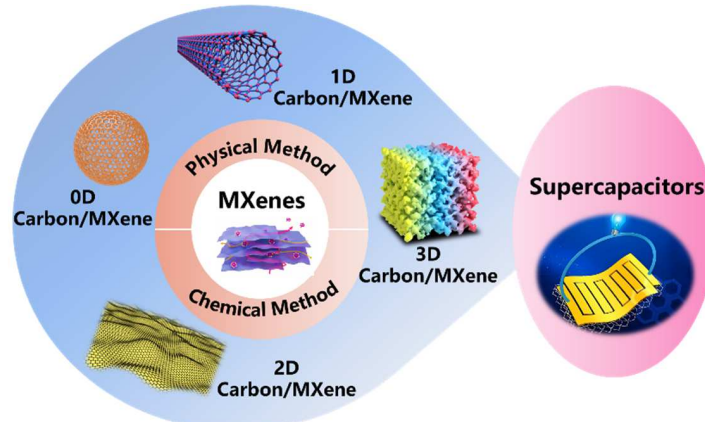


**Figure 1.** Schematic illustration of carbon/MXene composites for supercapacitors.

## 2. Synthesis of Carbon Materials/MXene Composites

### 2.1. Physical Method

Physical methods are the simplest way to prepare composite materials, and no new substances are formed during this process [38]. Moreover, this method enables the uniform mixing of various components of the material, thereby avoiding the complex steps and parameters that require strict control in the chemical reaction process [34]. At present, the physical synthesis strategies for carbon/Ti<sub>3</sub>C<sub>2</sub>T<sub>x</sub> composite materials include the mechanical mixing strategy, self-assembly strategy, vacuum-assisted filtration strategy, and some other preparation strategies.

#### 2.1.1. Mechanical Mixing Strategy

The mechanical mixing strategy utilizes techniques such as stirring, ball milling, and impregnation to uniformly crush or mix different components to form composite materials, which has the advantages of dependable and uncomplicated manipulation [18]. For carbon/MXenes composite materials, during the mechanical mixing process, MXenes can easily establish connections with other components due to the presence of abundant oxygen-containing functional groups [38]. Therefore, the strong interaction as a binding force between MXenes and the carbon structure forms a structurally stable carbon/MXenes composite material [38]. The carbon material as a conductive spacer is introduced into the intermediate layer of MXene nanosheets to form a mixed or sandwich structure, which will improve the performance by increasing the interlayer spacing, ion sites, and providing rapid ion transport [17]. Qi et al. prepared a flexible electrode of CC@MnO<sub>2</sub>@MXene by dipping methods so that MXene was completely coated on the CC@MnO<sub>2</sub> fiber surface [39]. When MXene is wrapped around the surface of CC@MnO<sub>2</sub>, it not only enhances the conductivity, but also generates more active sites of composite materials [39]. Accordingly, the composite materials provide a high charge storage performance, excellent cycling stability, and excellent energy density. Shi et al. designed a unique solvent-free ball-milling approach to prepare MOF/MXene composites, as shown in Figure 2a [40]. After selenization, metal selenides@carbon/MXene composite materials are prepared by transforming MOF/MXene. During this process, MXene is used as an electronic conductive network and form a mesoporous and macroporous structure of the obtained metal selenides@carbon/MXene composites [40].

### 2.1.2. Self-Assembly Strategy

The self-assembly process is the spontaneous aggregation of molecules, atoms, or nanomaterials into stable structures with certain regular shapes driven by electrostatic interactions, without any chemical bonds [19]. This method is simple and stable, and has been successfully applied to the synthesis of various composite materials. Due to the preparation process of etching and delamination, most MXenes have abundant surface functional groups (such as -O and -OH) [25]. Therefore, MXenes can easily and spontaneously aggregate with carbon materials to form stable and complete composites driven by electrostatic interactions, hydrogen bonds, and/or covalent bonds [18]. Fu et al. constructed graphene oxide/MXene (GO-M) composite materials using laser-induced electrostatic self-assembly technology, as shown in Figure 2b [41]. The GO-M in a reduced state prepared by the synergistic effect of a laser matter interaction and electrostatic self-assembly exhibits good conductivity and a layered micro/nano structure, which is significantly better than the reduced-state graphene oxide [41]. In addition, the introduction of MXenes makes the composite material rich in active sites, so the capacitance value achieved is five times that of the reduced graphene-based supercapacitors. Depijan et al. prepared  $\text{Ti}_3\text{C}_2\text{T}_x/\text{pg-C}_3\text{N}_4$  composite materials through self-assembly technology and the annealing process [42]. When pg- $\text{C}_3\text{N}_4$  is combined with  $\text{Ti}_3\text{C}_2\text{T}_x$ , the interlayer spacing and conductivity are effectively improved, and ion accessibility is enhanced. Therefore, the composite material exhibits excellent capacitance and cycling stability.

### 2.1.3. Vacuum-Assisted Filtration Strategy

The vacuum-assisted filtration strategy is used to prepare carbon/MXene composite materials through suction filtration and a pressure difference [34]. This method is simple, efficient, and widely used in the construction of carbon/MXene flexible electrodes. Due to the triple characteristics of metal-like conductivity, high mechanical properties, and surface functionality, MXenes can tightly bond with carbon materials to form flexible substrates during vacuum-assisted filtration processes without the need for additional polymer adhesives [19]. Hong et al. designed a DRCT-like CNT/ $\text{Ti}_3\text{C}_2$  composite through an alternate filtration process to integrate SACNT membranes with  $\text{Ti}_3\text{C}_2$  [43]. Benefiting from this biomimetic structure, the DRCT-like CNT/ $\text{Ti}_3\text{C}_2$  film could endure a mechanical strain of up to 8.01% and withstand 1000 cycles of extensive bending at angles of 90° and 180°. At room temperature, this anode delivered a high specific capacity and maintained a considerable capacity even after 3300 stable cycles. When subjected to a severe temperature of  $-40^\circ\text{C}$ , the DRCT-like CNT/ $\text{Ti}_3\text{C}_2$  anode still retained a substantial specific capacity. Yu et al. employed two-dimensional  $\text{Ti}_3\text{C}_2\text{T}_x$  MXene as a flexible, conductive, and electrochemically active binder for one-step vacuum-assisted filtration to prepare MXene-bonded activated carbon as a flexible electrode for supercapacitors, as shown in Figure 2c [44]. Yu et al. demonstrated a MXene-bonded activated carbon composite membrane using one-step vacuum-assisted filtration technology. The MXene layers encapsulate activated carbon particles to form a 3D conductive network, and 2D  $\text{Ti}_3\text{C}_2\text{T}_x$  MXene serves as a flexible, conductive, and electrochemically active adhesive. The synergistic effect of MXene and activated carbon expands the interlayer spacing, effectively improving the capacitance and rate capability of the composites, thus exhibiting a high capacitance of  $126 \text{ F g}^{-1}$  and a capacitance retention rate of 57.9% (0.1–100  $\text{A g}^{-1}$ ).

### 2.1.4. Other Strategies

Spray drying is a method of systematic technology applied to material drying [18]. During this process, when the solution is in contact with hot air, the solvent will vaporize rapidly to obtain dry powder or granular products. The particle size distribution and morphological structure can be adjusted flexibly by changing the process parameters such as the feed rate and viscosity of the solution [18]. Wang et al. presented a 3D lightweight porous microsphere composite (3D rGO/MXene/ $\text{TiO}_2/\text{Fe}_2\text{C}$ ) with a 2D/2D/0D/0D intercalation heterostructure by spray freeze-drying and microwave radiation, as shown in Figure 2d [45].

During the preparation process, defects, porous frameworks, multi-layer assemblies, and multi-component combinations are formed, effectively generating high-density polarized charges and abundant polarization sites, thus enhancing interfacial polarization [45].

Electrospinning is a simple and effective new processing technology for producing nanofibers and nanofiber-based materials [25]. In the electrospinning process, polymer solutions or melts are sprayed in a strong electric field. Due to the repulsive effect of charges, fibers will unfold and orient, while the solvent evaporates or solidifies, ultimately forming a fiber network [38]. This method has a high fiber orientation, controllable structure, and high production efficiency, making it easy to construct polymer solutions containing nanocomposites into fibers with adjustable properties [31]. Lei et al. prepared a  $\text{Ti}_3\text{C}_2\text{T}_x$  MXene/carbon nanofiber film using electrospinning technology, as shown in Figure 3a [46]. The number of active sites, electron/ion transport, and diffusion kinetics of the composite material have been effectively improved, resulting in a high desalination capacity, rapid desalination rate, and longer cycle life, which are superior to other carbon-based and MXene-based electrode materials [46].

The 3D printing strategy offers an advanced manufacturing technique that can easily create 3D structures by converting materials into ink, which can then be extruded through a nozzle and deposited layer by layer onto the substrate [47]. This technology can be directly printed into intersecting patterns of 3D microstructures [48]. By adjusting the process parameters, various desired morphological structures can be generated to meet more demands and achieve high efficiency. Dai et al. reported an MXene/RGO conductive scaffold using 3D printing technology, as shown in Figure 3b [48]. The addition of graphene oxide effectively improves the rheological and printability of MXene ink, ensuring the stability and structural integrity of conductive support connections. The improved ink has the flexibility of structural design and the adjustability of conformation, and the printed conductive scaffold has excellent reversible compressibility and excellent resistance to cyclic fatigue, which is significantly better than the reported MXene [48].

## 2.2. Chemical Method

### 2.2.1. Hydrothermal Strategy

The hydrothermal strategy, as one of the most common methods for preparing composites, refers to using an aqueous solution as the reaction medium in a specially designed closed-reaction vessel (autoclave), creating a high-temperature (100–1000 °C) and high-pressure (1–100 MPa) reaction environment through heating, so that usually slightly soluble or insoluble substances dissolve and recrystallize [38]. Zhu et al. developed a graphene-reinforced MXene hydrogel with 3D spherical macroporous structures (SGMH) by a hydrothermal reaction, as shown in Figure 3c [49]. In this configuration, graphene not only conductively assembles MXene sheets, but also improves the hydrophobicity of the composite hydrogel skeleton [49]. The stiffness and pore radius of SGMH are improved by the 3D spherical macroporous structures and prefreezing treatment, allowing it to be naturally dried and transition into graphene/MXene aerogel (SGMA) of arbitrary size scales [49]. Additionally, the 3D spherical structure inside the SGMA helps to homogenize the stress distribution and improve the electrical response during compression. Sangili et al. demonstrated a carbon-coated  $\text{Ti}_3\text{C}_2\text{T}_x$  MXene ( $\text{Ti}_3\text{C}_2\text{T}_x@\text{C}$ ) by a hydrothermal method [50]. Surface oxidation and aggregation can be effectively inhibited by the *in situ* wrapping of  $\text{Ti}_3\text{C}_2\text{T}_x$  in carbon layers, enabling the composite to be stored in water and air for 100 days. Moreover, the composite material exhibits high capacitance and long-term cycling stability.

### 2.2.2. Heat Treatment Strategy

In addition to the hydrothermal method, the heat treatment strategy is another commonly used method for preparing composite materials. In the heat treatment process, the microstructure and phase state of the materials are changed by controlling the heating and cooling process, so as to improve the crystal structure, eliminate defects, and improve the performance of the materials [38]. Allah et al. reported a  $\text{Ti}_3\text{C}_2\text{T}_x$ -NOMC heterostructure

(composed of  $\text{Ti}_3\text{C}_2\text{T}_x$  and nitrogen-doped ordered mesoporous carbon) through heat treatment techniques [51]. The introduction of abundant ordered mesoporous NOMC on the surface of  $\text{Ti}_3\text{C}_2\text{T}_x$  nanosheets with high electronic conductivity can suppress stacking and aggregation phenomena, prevent oxidation, increase ion transport pathways, and efficiency. Therefore, the material exhibits an excellent capacitance value, rate performance, and cycle life. Zhang et al. proposed a heat treatment technique for directly preparing 3D carbon-coated  $\text{Ti}_3\text{C}_2\text{T}_x$  composite materials (T-MXene@C) in Figure 3d [52]. The composite material presents a 3D silver ear-like structure, and a thin carbon coating completely covering the surface of  $\text{Ti}_3\text{C}_2\text{T}_x$  nanosheets, thus inhibiting oxidation and aggregation. This structure endows the composite material with a stable and rich active surface, effectively improving the charge transfer rate, and achieving an ultra-high capacity and an excellent rate performance and cycle life.

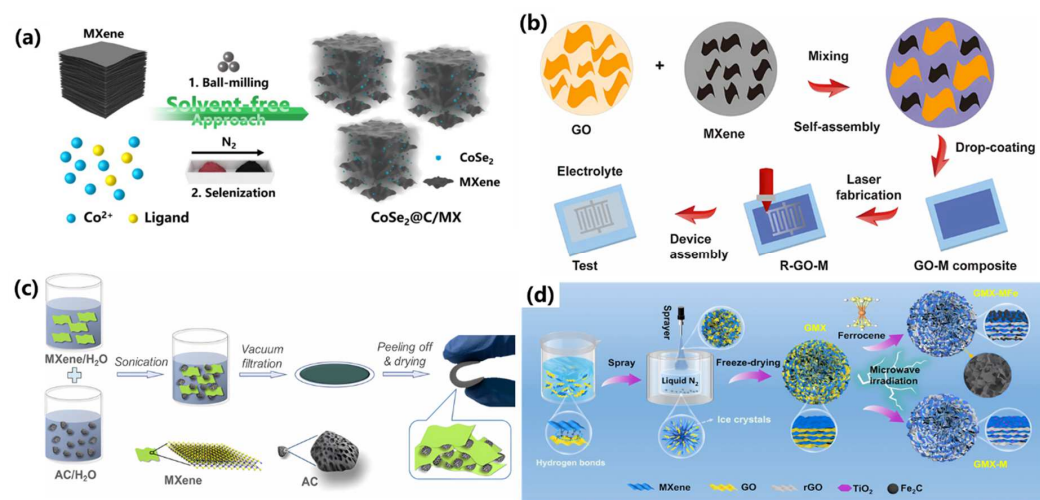


**Figure 2.** Physical method for the fabrication of carbon/MXene composites: Schematic diagram of (a) selenides@carbon/MX [40], copyright 2023, Elsevier, (b) GO-M [41], copyright 2023, American Chemical Society, (c) AC/MXene [44], copyright 2018, American Chemical Society, and (d) rGO/MXene/TiO<sub>2</sub>/Fe<sub>2</sub>C [45], copyright 2023, Springer.

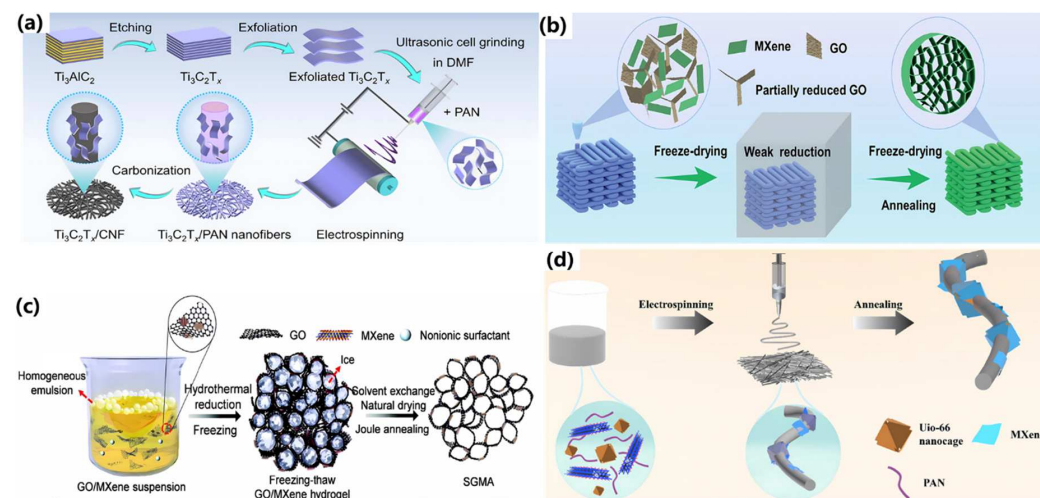


**Figure 3.** Physical method for the fabrication of carbon/MXene composites: (a) Schematic diagram of  $\text{Ti}_3\text{C}_2\text{T}_x/\text{CNF}$  [46], copyright 2023, Royal Society of Chemistry, and (b) MXene/RGO [48], copyright 2022, Royal Society of Chemistry. Chemical method for the fabrication of carbon/MXene composites: (c) Schematic diagram of SGMA [49], copyright 2024, Wiley-VCH GmbH, and (d) T-MXene@C [52], copyright 2024, Elsevier.

### 3. Carbon Materials/MXenes Composites for Supercapacitors

Combining carbon materials and MXenes to build a composite material can take full advantage of the advantages of both materials to achieve “1 + 1 > 2”, thus significantly improving the performance of supercapacitors [19,53]. Firstly, the excellent electrical conductivity of MXenes can effectively improve the electrical conductivity of porous carbon materials, thereby improving the overall electrical conductivity of the electrode [23,54]. The introduction of carbon materials can increase the interlayer spacing of MXene nanosheets, effectively alleviating the occurrence of stacking and re-aggregation phenomena [25,55]. In addition, carbon materials can contribute more storage sites, thereby improving their energy storage capacity [17,56]. Currently, MXenes have been used to construct composite materials with carbon materials of various sizes (0–3D), and have significantly improved the electrochemical performance.

#### 3.1. Zero-Dimensional Carbon/MXenes Composites

Zero-dimensional carbon materials mainly refer to carbon quantum dots (CQDs), which are a promising low-dimensional nanomaterial [19,57]. CQDs have excellent electronic conductivity and high carrier mobility, which makes them stand out in electronic devices [58]. In addition, CQDs have excellent chemical and environmental stability and are considered environmentally friendly nanomaterials [23]. At the microscale, compared to other quantum dots, CQDs typically exhibit a spherical structure filled with sp<sub>2</sub> and sp<sub>3</sub> hybridized carbons, possessing an overall smaller size (<10 nm) [25]. CQDs containing abundant surface functional groups (such as carboxyl and hydroxyl groups) can provide satisfactory water solubility, and enable CQDs to assemble with MXene at liquid–liquid interfaces [19]. In recent years, CQDs have become a typical carbon material combined with MXene to construct composite materials. Small-sized CQDs can be dispersed on the plane of MXene to prevent nanosheets re-stacking, expose more active sites, and promote electrolyte diffusion within MXene nanosheets [58]. When MXene/CQDs composite materials are used as electrode materials, they have a high specific capacitance and capacitance retention ability, achieving an increase in the energy density of supercapacitors. Wang et al. reported an MXene/carbon dot (p-MC) composite film with a 3D interconnected porous structure [59]. Carbon dots are inserted between MXene nanosheets to prevent re-stacking and aggregation, achieving the generation of more electrochemical active sites. The macropores in 3D porous structures facilitate efficient ion diffusion, and the interlayer pore structure rapidly transfers ions to active sites to participate in reactions. Therefore, the high weight capacitance (688.9 F g<sup>-1</sup> at 2 A g<sup>-1</sup>) and excellent rate performance are achieved for p-MC films. Zhang et al. proposed an MXene/CAC (calcium alginate-derived carbon dots) composite film with a large ion accessible active surface and high density through carbon dot intercalation technology, as shown in Figure 4a–d [60]. Carbon dots embedded into MXene nanosheets increase interlayer spacing and facilitate the efficient diffusion of ions in the electrolyte. Therefore, the composite film exhibits a high-volume capacitance value of 1244.6 F cm<sup>-3</sup>, excellent rate capacity of 53.2% (1–1000 A g<sup>-1</sup>), and cycling stability (93.5% after 30,000 cycles).

Besides CQDs, 0D porous carbon microspheres are also expected to become conductive spacers, promoting electrolyte migration kinetics and improving the electrochemical performance. Wei et al. fabricated a porous carbon spheres/MXene composite (CPCM/MXene) with a sandwich-like structure through electrostatic interactions between a Ti<sub>3</sub>C<sub>2</sub>T<sub>x</sub> MXene and chitosan-based porous carbon microsphere [61]. The spherical structure of CPCM is protected by Ti<sub>3</sub>C<sub>2</sub>T<sub>x</sub>, while CPCM inhibits the re-aggregation of Ti<sub>3</sub>C<sub>2</sub>T<sub>x</sub> nanosheets, achieving an improvement in electrolyte migration kinetics. Driven by the synergistic effect, PCM/MXene exhibits a specific capacitance value of 362 F g<sup>-1</sup> and a capacitance retention rate of 93.87% after 10,000 cycles. Yang et al. designed a composite film (MXene/MHCS/CNT) composed of hollow carbon spheres (MHCS)/MXenes heterostructures and carbon nanotubes, as shown in Figure 4e–g [62]. This structure and design effectively increase the specific surface area, pore structure, stability, and conductivity of

the composite material, thus achieving the improved penetration efficiency of the electrolyte solution and a shortened ion transport process. Therefore, the excellent specific capacitance value of  $395 \text{ F g}^{-1}$ , rate performance of 70.9% (2–1000 mV s $^{-1}$ ), and cycling stability (98.3% after 10,000 cycles) exist.

Zero-dimensional carbon materials can serve as an intercalation agent for MXenes, and carbon materials can also form 0D structures with MXenes to enhance electrochemical performance. Li et al. demonstrated a hollow core–shell microsphere ( $\text{NiCo}_2\text{S}_4/\text{MXene/NC}$ ) composed of  $\text{NiCo}_2\text{S}_4$ , MXene, and N-doped carbon through a multi-step process, as shown in Figure 4h–k [63]. The introduction of MXene and N-doped carbon materials effectively improves the conductivity of the composite material, while the special hollow structure can suppress the occurrence of unstable factors during the charge and discharge processes. Therefore, the electrode based on the composite material exhibits excellent capacitance ( $1786 \text{ F g}^{-1}$ ) and cycling stability (over 100% after 10,000 cycles). Moreover, the corresponding hybrid supercapacitor devices can achieve a maximum energy density of  $67 \text{ Wh kg}^{-1}$  and a capacitance retention rate of over 80% after 10,000 cycles.

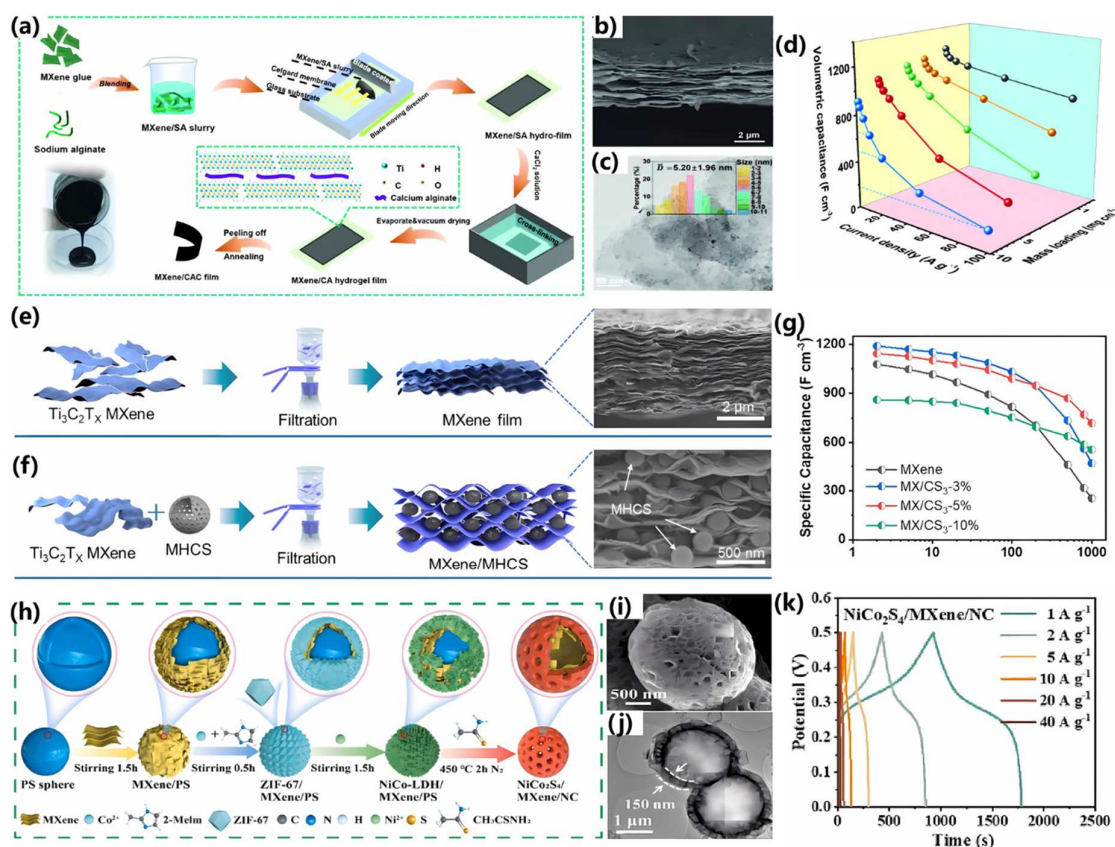


**Figure 4.** Zero-dimensional carbon/MXene composites: (a) Schematic diagram, (b) SEM, (c) TEM, and (d) capacitance value of MXene/CAC films [60], copyright 2022, Wiley-VCH GmbH. Schematic diagram of (e) pure MXene film and (f) MXene/MHCS film, (g) capacitance value [62], copyright 2024, Elsevier. (h) Schematic diagram, (i) SEM, (j) TEM, and (k) GCD curves of  $\text{NiCo}_2\text{S}_4/\text{MXene/NC}$  [63], copyright 2024, Elsevier.

### 3.2. One-Dimensional Carbon/MXenes Composites

One-dimensional carbon materials typically include nanotubes, nanofibers, or nanoribbons. For example, carbon nanotubes (CNTs) have the advantages of a high mechanical strength, low electrical resistivity, strong conductivity, large specific surface area, good chemical stability, good contact with electrolytes, and their “tubular” structure and higher aspect ratio can provide sufficient high-speed channels for an electron transfer [18,19,64]. Compared to 0D CQDs, the interaction between carbon nanotubes can spontaneously form

a highly conductive network, which can be used as a self-supporting material without binders or substrates [23]. More importantly, most nanomaterials with a 1D structure typically have a relatively high mechanical strength to realize a sturdy structure [25]. Therefore, 1D carbon materials are highly suitable as “spacers” to introduce in a 2D MXene nanosheet, stabilize the structure of composite materials, and help further alleviate or avoid self-stacking re-aggregation phenomena [17]. Various structures can be established by coupling 1D carbon-based materials at the nanoscale with 2D MXene through different synthesis or assembly methods.

One-dimensional CNT can grow spontaneously on 2D MXene nanosheets to form a “1D tube on a 2D sheet” pattern through chemical vapor deposition (CVD) or catalytic conversion. Therefore, the interaction between 1D CNT and 2D MXenes is relatively strong, usually resulting in a lower contact impedance [19]. Wang et al. designed MXene/N-CNT composite materials with a hierarchical porous structure that effectively suppressed the self-accumulation of 2D MXene and 1D N-CNT, as shown in Figure 5a–c [65]. This structure increases the interlayer spacing of MXene and the specific surface area of the composite material, obtaining more active sites to participate in reactions and ion diffusion channels. The composite material exhibits a significantly better specific capacitance ( $167.2 \text{ F g}^{-1}$ ) than the original MXene electrode. Moreover, the asymmetric supercapacitor device based on this composite material has a high capacitance retention rate of 73.2% after 10,000 cycles, a high Coulombic efficiency of 97.5%, and a maximum energy density of  $12.1 \text{ Wh kg}^{-1}$ . Li et al. reported an *in situ* growth of multi-walled carbon nanotubes on MXene nanosheets loaded on a CC (MWCNTs-MXene@CC) composite material, achieving a synergistic combination of a large surface area and excellent electrical conductivity [66]. The growth of MWCNTs on MXene nanosheets can not only effectively suppress the occurrence of re-stacking phenomena, but also serve as charge collectors within and between nanosheets. Based on the 3D interconnected structure and high specific surface area of the composite material, rapid electrolyte penetration and efficient charge collection have been promoted, thus achieving an area-specific capacitance of  $114.58 \text{ mF cm}^{-2}$  and a high-capacity retention rate of 118%, which is significantly better than early-reported MWCNTs and MXene composite materials.

Hydrogen bonding, as a classic electrostatic interaction, is also considered an important bridge for achieving microscale structural integration. The surface of 2D MXenes contains abundant surface functional groups (-OH, -F, etc.), which can effectively participate in hydrogen bonding to construct composite materials by combining MXenes with 1D tubular carbon nanomaterials with rich surface chemical properties [64]. Hakim et al. grafted MWCNTs and  $\text{Mo}_2\text{TiC}_2\text{T}_x$  to construct a composite (MWCNTs@ $\text{Mo}_2\text{TiC}_2\text{T}_x$ ), which achieved a significant improvement in electrochemical properties and reaction kinetics [67]. MWCNT as a conductive medium is introduced into MXene, which effectively improves the specific surface area and conductivity of the composite material, achieving a capacitance value of  $1740 \text{ F g}^{-1}$ , almost four times that of the original  $\text{Mo}_2\text{TiC}_2\text{T}_x$ . You et al. reported a hybrid carbon nanofiber membrane (MCNF) derived from MXene/polyacrylonitrile, as shown in Figure 5d–f [68]. As the content of MXene nanosheets increases, the deposition thickness continuously increases and uniformly adheres to the surface of CNFs, which enhances the hydrophilicity of MCNF. Therefore, the electrolyte permeability at the electrode–electrolyte interface is improved, achieving the specific capacitance of  $436.5 \text{ F g}^{-1}$ , significantly better than that of pure CNFs.

When the size of 1D carbon-based materials increases to a size larger than that of 2D MXene nanosheets, smaller 2D MXene nanosheets will randomly deposit or be located on the surface of 1D carbon-based materials, forming a “2D on 1D” structure [19]. Sun et al. prepared a heterostructure of MXene/biomass-derived carbon fiber (MXene/CF) with a hierarchical porous “skin/skeleton”-like structure, which effectively suppressed the stacking and re-aggregation of MXene nanosheets, as shown in Figure 6a–c [69]. This structure enhances the electrolyte penetration rate, allowing ions to rapidly diffuse/transfer into the electrode due to efficient and stable channels. Therefore, the composite material exhibits an excellent volumetric capacitance of  $7.14 \text{ F cm}^{-3}$ , rate characteristics of 63.9%

( $0.5\text{--}100 \text{ A g}^{-1}$ ), and cycling stability (99.8% after 5000 cycles). The all-solid state symmetrical supercapacitor device based on this composite material not only exhibits an excellent electrochemical performance, but also can withstand 2500 cycles under different bending conditions. Dharmasiri et al. developed a MXene-coated carbon fiber (CF) composite material with a stable structure and excellent mechanical performance, exhibiting a specific capacitance of  $157 \text{ F g}^{-1}$ , which is approximately 725 times higher than the original non-functionalized CF [70]. When applied to functionalized and coated woven CF pads and used to construct supercapacitor devices, a specific capacitance of  $908 \text{ mF g}^{-1}$  was achieved, which is approximately 42 times that of the control group.

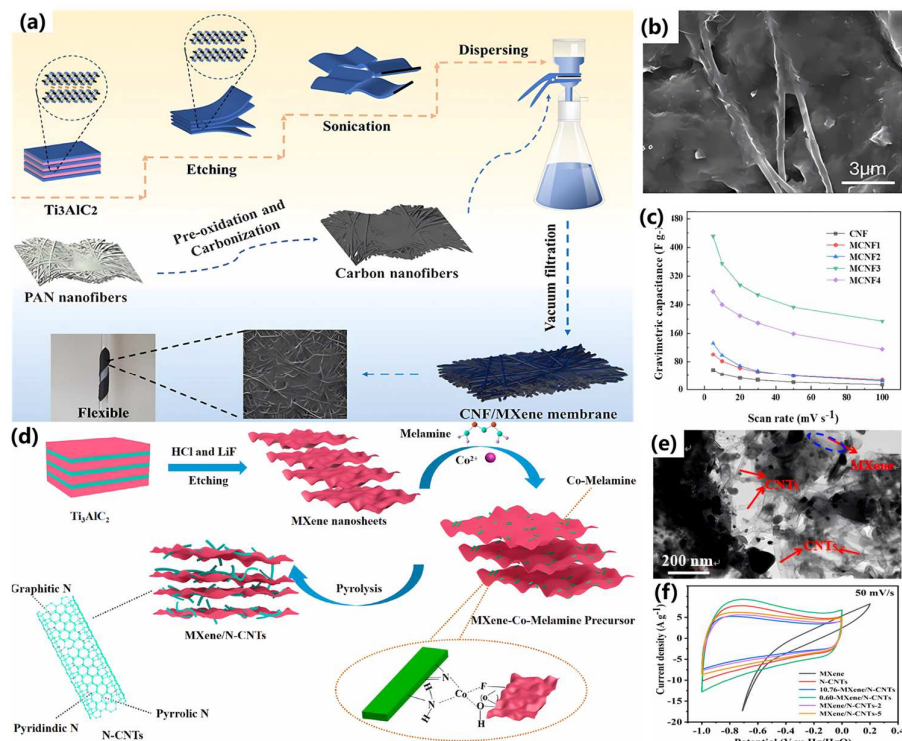


**Figure 5.** One-dimensional carbon/MXene composites: **(a)** Schematic diagram, **(b)** SEM, and **(c)** capacitance value of MXene/N-CNT [65], copyright 2023 American Chemical Society. **(d)** Schematic diagram and **(e)** TEM of MCNFs, **(f)** CV curves [68], copyright 2024, Springer.

Transforming the hybrid mode of 1D carbon materials/2D MXene into nanotube or nanofiber structures is also a method that can fundamentally avoid the overlap phenomenon of 2D MXene nanosheets, named “2D to 1D” [23]. Song et al. integrated MXene into N-doped carbon nanofibers with cavity-interconnected porous structures to construct a composite carbon film [71]. This design and structure expose more active sites, exhibiting a significantly enhanced electrochemical performance, such as a maximum energy density of  $26.2 \text{ Wh kg}^{-1}$  and a capacitance retention rate of 96.3% after 10,000 cycles. Zhao et al. developed a multifunctional  $\text{Ti}_3\text{C}_2\text{T}_x$  MXene/carbon nanotube (MXene/CNT) hybrid fiber through the wet spinning strategy, as shown in Figure 6d–f [72]. When the CNT content is about 1 wt%, the mixed fiber can achieve a high strength of  $61 \pm 7 \text{ MPa}$ , a conductivity of  $1142.08 \pm 40.04 \text{ S cm}^{-1}$ , and an excellent specific capacitance of about  $295 \text{ F g}^{-1}$ . As the load increases to 9wt%, a maximum strain of  $161 \pm 19 \text{ MPa}$  and further increased conductivity ( $1715 \pm 22 \text{ S cm}^{-1}$ ) can be achieved. Therefore, the MXene/CNT fibers can be woven into energy storage textiles due to the excellent mechanical properties and achieve a maximum energy density of approximately  $6.08 \text{ mW h cm}^{-3}$ .

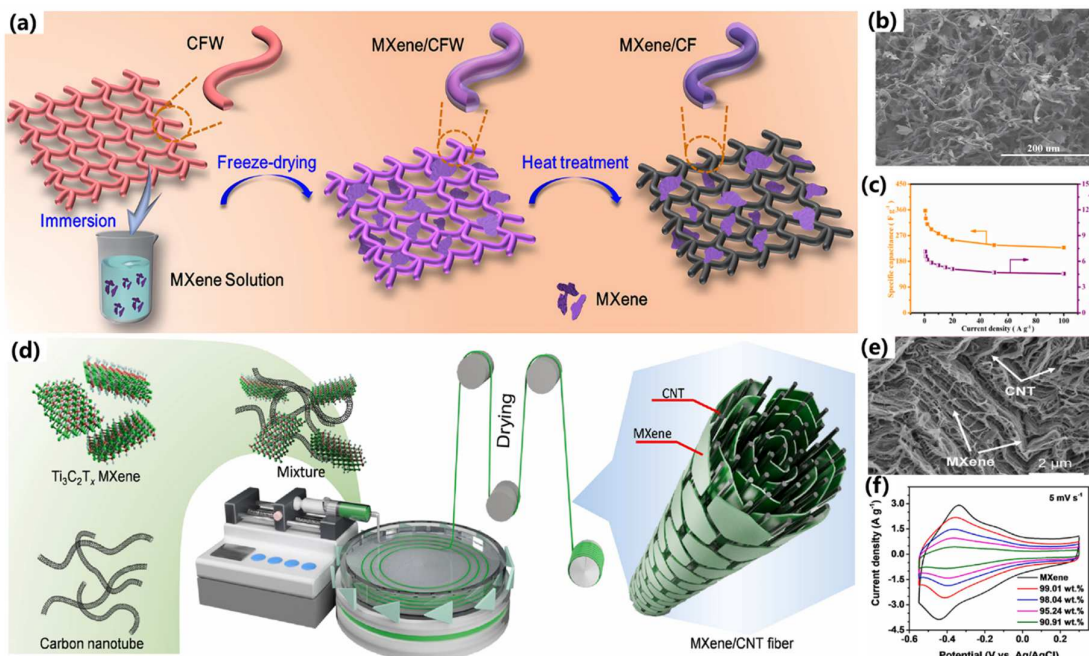


**Figure 6.** One-dimensional carbon/MXene composites: (a) Schematic diagram, (b) SEM, and (c) Capacitance value of MXene/CF [69], copyright 2020, Elsevier. (d) Schematic diagram and (e) TEM of MXene/CNT fiber, (f) CV curves [72], copyright 2022, Elsevier.

### 3.3. Two-Dimensional Carbon/MXenes Composites

Two-dimensional carbon materials have the characteristics of a large specific surface area, high electrical conductivity, high stability, and excellent mechanical properties [25]. Different forms of 2D carbon materials' (graphene, g-C<sub>3</sub>N<sub>4</sub>, carbon nanosheets, etc.) composite materials have been constructed in combination with MXene for applications in supercapacitors and have shown excellent electrochemical properties.

As a typical two-dimensional material, graphene is composed of a single-atom-thick carbon layer, which has unique properties beyond 0D and 1D carbon materials; these include strong in-plane covalent bonds with high conductivity, a suitable layer thickness and a wide transverse size that shortens the ion transport path, and large exposed surfaces that facilitate ion adsorption [19,73]. The surface portion of functionalized graphene serves as an oxidation-reduction center, making a significant contribution to Faradaic-type capacitors [19]. Similar to MXene, graphene nanosheets also exhibit self-aggregation. However, the introduction of graphene into MXene will inhibit the defects of the two materials, and achieve a synergistic effect to enhance the electrochemical properties [19]. Dang et al. constructed a reduced graphene oxide/Ti<sub>3</sub>C<sub>2</sub>T<sub>x</sub>/carbon nanotube (rGO/Ti<sub>3</sub>C<sub>2</sub>T<sub>x</sub>/CNT) fiber [74]. This composite material effectively suppresses stacking and aggregation phenomena through π–π stacking interactions, hydrogen bonding, and van der Waals forces. Moreover, all solid-state supercapacitor devices based on this material composite show a high-volume capacitance (336.1 F cm<sup>-3</sup>) after 3000 cycles and a high-volume energy density of 23.11 mWh cm<sup>-3</sup>. Qin et al. designed and prepared a nanofiber-reinforced MXene/rGO conductive aerogel by the pyrrole-assisted hydrothermal reduction of GO nanosheets, as shown in Figure 7a–d [75]. Pyrroles can not only induce the reduction of GO and self-assemble into an ordered 3D porous structure, but also in situ polymerized polypyrrole (PPy) can achieve strong cross-linking between rGO and MXene nanosheets through covalent and noncovalent bonds [75]. Meanwhile, the introduction of hydroxyl-rich cellulose acetate (CA) nanofibers into the aerogel to construct a “brick-mortar-rebar” structure can endow the material with excellent mechanical properties [75]. The conductive MXene/rGO aerogel served as a supercapacitor electrode and made full use of the electric double-layer capacitance of rGO and the Faradaic-type capacitors of MXene and PPy to

store energy. The porous structure can effectively solve the problem of restacking, facilitate the rapid diffusion of ions in the electrode materials, and demonstrate potential applications in energy storage [75]. The all-solid-state supercapacitor based on MXene/rGO aerogel is also fabricated, which shows a high area-specific capacitance of up to  $274 \text{ mF cm}^{-2}$  at a current density of  $1 \text{ mA cm}^{-2}$ .

Graphite nitride carbon ( $\text{g-C}_3\text{N}_4$ ) is a kind of carbon material with a high nitrogen content and a typical polymer semiconductor, which has a two-dimensional layered structure similar to graphene, high electrochemical reactivity, surface polarity, and wettability [25]. The pyridine type N atom in  $\text{g-C}_3\text{N}_4$  acts as an active site, making it prone to highly reversible chemical reactions with electrolyte ions [76]. Therefore, the introduction of  $\text{g-C}_3\text{N}_4$  into MXene can not only achieve the effective inhibition of a nanosheet stack, but also improves the electrochemical properties of the materials. Xu et al. reported an *in situ* synthesis technique for a  $\text{g-C}_3\text{N}_4/\text{TiVCT}_x$  composite material [77]. The coating of  $\text{g-C}_3\text{N}_4$  on  $\text{TiVCT}_x$  nanosheets can effectively inhibit the occurrence of oxidation and self-stacks, so that the composite still maintains a high specific capacitance of  $508.9 \text{ F g}^{-1}$  after 7000 cycles. Zhang et al. constructed a  $\text{Ti}_3\text{C}_2\text{T}_x/\text{g-C}_3\text{N}_4$  heterostructure by the self-assembly method, which avoids stacking, increases layer spacing, and enhances the charge transfer efficiency, as shown in Figure 7e–g [78]. This composite material exhibits a specific capacitance value of  $414 \text{ F g}^{-1}$ , and the assembled supercapacitor device can not only maintain a stable performance under  $180^\circ$  bending conditions, but can also achieve a maximum energy density of  $23.98 \text{ Wh kg}^{-1}$ .

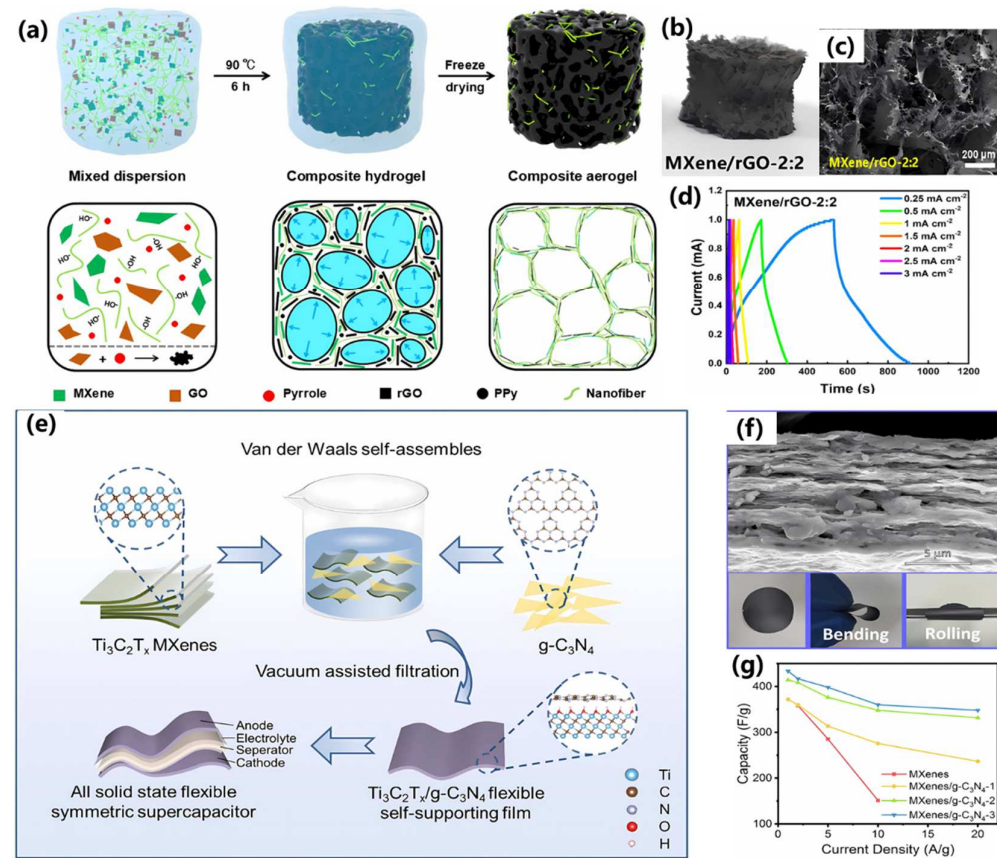


**Figure 7.** Two-dimensional carbon/MXene composites: (a) Schematic diagram, (b) Photograph, (c) SEM, and (d) GCD curves of MXene/rGO aerogel [75], copyright 2024, American Chemical Society. (e) Schematic diagram and (f) SEM of  $\text{Ti}_3\text{C}_2\text{T}_x/\text{g-C}_3\text{N}_4$  heterostructure, (g) capacitance value [78], copyright 2022, Elsevier.

Carbon nanosheets have a two-dimensional sheet-like structure with many unique physical and chemical properties and potential applications, such as a high specific surface

area providing more reaction sites, excellent conductivity allowing for very fast electron migration, excellent chemical stability, resisting oxidation and reduction reactions, high mechanical strength, etc., [79]. The 2D/2D composite materials constructed by combining carbon nanosheets with MXenes have large interlayer pores, high conductivity, structural stability, etc., which is conducive to electron transfers and electrode lifetime enhancement, while maintaining the unique crystal structure and characteristics of MXenes [80]. Moreover, the introduction of carbon nanosheets can provide a sufficient porous structure inside the intermediate layer, suppressing the stacking and aggregation of MXene nanosheets [79]. Zhang et al. prepared a composite material (MXene/CCNS) composed of MXene and citrus-derived carbon nanosheets, which can serve as a flexible self-supporting electrode to achieve a high specific capacitance of  $1825.6 \text{ mF cm}^{-2}$  and a capacity retention rate of 99.82% after 10,000 cycles [79]. Moreover, the composite material can be configured for conductive ink screen printing and large-scale patterned electrodes, respectively achieving a capacitance and energy density of  $114.9 \text{ mF cm}^{-2}$  and  $12.9 \mu\text{Wh cm}^{-2}$  for the application of forked supercapacitors, which constructed a composite material (MCN) by inserting high nitrogen-doped carbon nanosheets (CN) into MXene, as shown in Figure 8a–c [80]. This design effectively suppresses the occurrence of the MXene stacking phenomenon and improves the stability of the structure and ion transport efficiency. The doping of heteroatoms N achieves the control of the electronic structure of the composite materials and contributes to the Faraday capacitance, demonstrating a high specific capacitance of  $418.4 \text{ F g}^{-1}$ .

Apart from graphene,  $\text{g-C}_3\text{N}_4$ , and carbon nanosheets, graphdiyne (GDY), as an emerging two-dimensional carbon material, has rich carbon chemical bonds, large conjugated systems, wide interplanar spacing, and excellent chemical stability [81]. GDY is a novel all-carbon framework with a unique  $\pi$ -conjugated  $\text{sp}^2$  and  $\text{sp}$ -hybrid backbone and a macroporous structure [82]. When GDY is grown *in situ* on the surface of MXene, the intercalation capacitance behavior and bulk energy density can be improved by increasing the nanosheet spacing and active sites to effectively promote ion migration dynamics/storage and interfacial electron conduction [83]. Wu et al. reported a hydrogen-rich GDY- $\text{Ti}_3\text{C}_2\text{T}_x$  electrode, which achieved the effective regulation of layer spacing, active sites, and charge storage, as shown in Figure 8d–f [83]. Due to the strong H + electrostatic attraction, low migration resistance, accelerated intercalation pseudocapacitance dynamics, fast electron response, and stable Ti-O-C bond bridge organic–inorganic heterojunction, the composite exhibits a short-range electron transport pathway, high ion diffusion rate, and electrolyte permeation, resulting in a volume capacitance of  $2296 \text{ F cm}^{-3}$ , 55% rate characteristics ( $1\text{--}50 \text{ A cm}^{-3}$ ), a volume energy density of  $65.6 \text{ mWh cm}^{-3}$ , and long-term deformable cycling stability.

### 3.4. Three-Dimensional Carbon/MXenes Composites

Three-dimensional carbon materials typically have interconnected porous structures that provide large electrochemical active surface areas and excellent electron and mass transfer capabilities [23]. Compared with 0D, 1D, and 2D carbon materials, 3D carbon materials have unique advantages. When combined with two-dimensional MXene layers, the composite materials exhibit excellent physical and chemical properties and demonstrate an outstanding performance in the field of energy storage [17]. Under the premise of a reasonable nanostructure design, carbon materials and MXene exert synergistic effects in 3D/2D composite materials to achieve satisfactory results [19]. In view of the difference in size, 3D carbon materials and MXenes can combine to build composite materials with different structures, such as activated carbon or hierarchical porous carbon embedded in the MXene layer and MXenes deposited on the surface of carbon cloth and carbon foam.

Activated carbon with advantages such as a large specific surface area, good electrical performance, global availability, biodegradability, and low cost is the earliest electrode material used in supercapacitors [17]. The physical or chemical activation process can not only make the specific surface area of activated carbon up to  $3000 \text{ m}^2 \text{ g}^{-1}$ , but also build

a porous structure, which is conducive to combining with various materials to construct composite materials, thereby improving the electrochemical performance [23]. A group studied a composite material of tin (IV) selenide ( $\text{SnSe}_2$ ) growth and inserted activated porous carbon/ $\text{Ti}_3\text{C}_2\text{T}_{\text{x}}$  (APC/MXene), as shown in Figure 9a–c [84]. The highly porous APC structure wrapped in  $\text{Ti}_3\text{C}_2\text{T}_{\text{x}}$  effectively suppresses the occurrence of re-stacking and exposes more active sites. Therefore, the composite material as an electrode material has a high capacitance value of  $815 \text{ F g}^{-1}$ , and the assembled supercapacitor device achieves a maximum energy density of  $102 \text{ Wh kg}^{-1}$ . Yong et al. reported two methods for combining MXene ( $\text{Ti}_3\text{C}_2\text{T}_{\text{x}}$ ) with activated carbon (AC) to construct porous, flexible, and mechanically durable composite films, including multilayer MXene powder deposited on textiles after mechanical mixing with AC pulp, and MXene nanosheets sprayed on the surface of sprayed AC electrodes, achieving the optimal specific capacitance of  $148.7 \text{ mF cm}^{-2}$  and an energy density of  $0.921 \text{ mW cm}^{-2}$  [85]. Compared with identical supercapacitors with standard AC electrodes, the composite prepared by combining these two methods has a 220% increase in capacitance.

In addition to activated carbon, hierarchical porous carbon also has unlimited potential to be combined with MXenes to construct composite materials, achieving high chemical stability, an adjustable porous structure, and a specific surface area [23]. Hou et al. reported a porous heterostructure of MXenes/waste PET-derived carbon, as shown in Figure 9d–f [86]. Carbon materials in composite materials inhibit the re-aggregation of  $\text{Ti}_3\text{C}_2\text{T}_{\text{x}}$ , while  $\text{Ti}_3\text{C}_2\text{T}_{\text{x}}$  increases the electrochemical active sites. The large specific surface area ( $1754.3 \text{ m}^2 \text{ g}^{-1}$ ) promotes electrolyte migration kinetics and achieves a high specific capacitance value ( $404.1 \text{ F g}^{-1}$ ). The supercapacitor device based on this composite material has a voltage window of  $1.8 \text{ V}$ , energy density of  $31.19 \text{ Wh kg}^{-1}$ , and 1% capacitance decay after 15,000 cycles. Seenath et al. demonstrated an MXene-coupled nitrogen-doped porous carbon (MX-MC-N) hybrid material with a high specific surface area ( $796 \text{ m}^2 \text{ g}^{-1}$ ) and hierarchically porous networks, achieving an effective improvement in the electrochemical performance [87]. The composite material has a high capacitance value of  $245 \text{ F g}^{-1}$ , which is significantly better than porous carbon without MXene, graphene, and nitrogen-doped porous carbon materials. In addition, the symmetrical and asymmetrical supercapacitors based on this composite material exhibit high areal capacitance values of  $72 \text{ mF cm}^{-2}$  and  $228 \text{ mF cm}^{-2}$  and an energy density of  $13 \mu\text{Wh cm}^{-2}$  and  $92.1 \mu\text{Wh cm}^{-2}$ , respectively.

Some organic compounds (glucose, citric acid, lignin, etc.) can be used as carbon sources to construct carbon/MXene composites with 2D MXene nanosheets [19,23,25]. Huang et al. reported a composite material (N, S-MXene/3DPC) composed of N and S co-doped 3D porous carbon and MXene, achieving a specific capacitance of  $412.7 \text{ F g}^{-1}$  [88]. The 3D conductive network co-doped with N and S can provide multiple transport paths and abundant translation active sites for ions and charges, while avoiding MXene stacking. The introduction of MXene effectively improves the conductivity and mechanical stability. Therefore, the asymmetric supercapacitor based on the material has a capacitance value of  $210.5 \text{ F g}^{-1}$ , 97.5% capacitance retention after 5000 cycles, and a maximum energy density of  $94.7 \text{ Wh kg}^{-1}$ . Yang et al. prepared a highly conductive  $\text{Ti}_3\text{C}_2\text{T}_{\text{x}}/\text{CNT}/\text{PC}$  composite film by tightly anchoring porous carbon (PC) onto MXene nanosheets using 1D CNT as a bridge, as shown in Figure 9g–i [89]. The composite material exhibits a high specific capacitance of  $364.8 \text{ mF cm}^{-2}$ , an over 80% rate performance ( $0.5\text{--}50 \text{ mA cm}^{-2}$ ), and a large area energy density of  $10.5 \mu\text{Wh cm}^{-2}$ .

When the size of the 3D structural skeleton is larger than that of the 2D MXene nanosheets, the 2D MXene nanosheets are located on the surface or surfaces of the 3D carbonaceous skeleton, forming a “2D in 3D” mode. Highly porous 3D carbonaceous frameworks are typically prepared by the high-temperature carbonization of natural biomass or inherently porous structured polymers. Yao et al. prepared a super-high mechanical strength and self-supporting carbonized wood (CW)/MXene nanocomposite material, which not only prevented the re-aggregation of MXene, but also fully utilized the dual effects of CW (a graded porous structure) and MXene (high conductivity and wettability).

ity) [90]. Therefore, the symmetrical supercapacitor based on this composite material exhibits a high capacitance characteristic of  $4.24 \text{ F cm}^{-2}$  ( $80.61 \text{ F g}^{-1}$ ) and a high energy density of  $11.2 \text{ Wh kg}^{-1}$ . Sun et al. prepared a new type of MXene/N-doped carbon foam (MXene/NCF) compressible composite with a 3D hollow interconnection structure, as shown in Figure 10a–d [91]. NCF can provide additional pseudocapacitance through N atom doping, while supporting MXene nanosheets to form 3D hollow interconnected structures, providing highly stable and efficient channels and more contact sites for ion diffusion/electron transport. MXene enhances the conductivity and hydrophilicity of composite materials. Due to the synergistic effect, the composite material exhibits high capacitance characteristics of  $332 \text{ F g}^{-1}$  ( $3162 \text{ mF cm}^{-3}$ ), a 64% rate performance ( $0.5\text{--}100 \text{ A g}^{-1}$ ), and 99.2% capacity retention after 10,000 cycles. In addition, the material can withstand multiple 60% strains with a stable morphology and electrochemical properties.

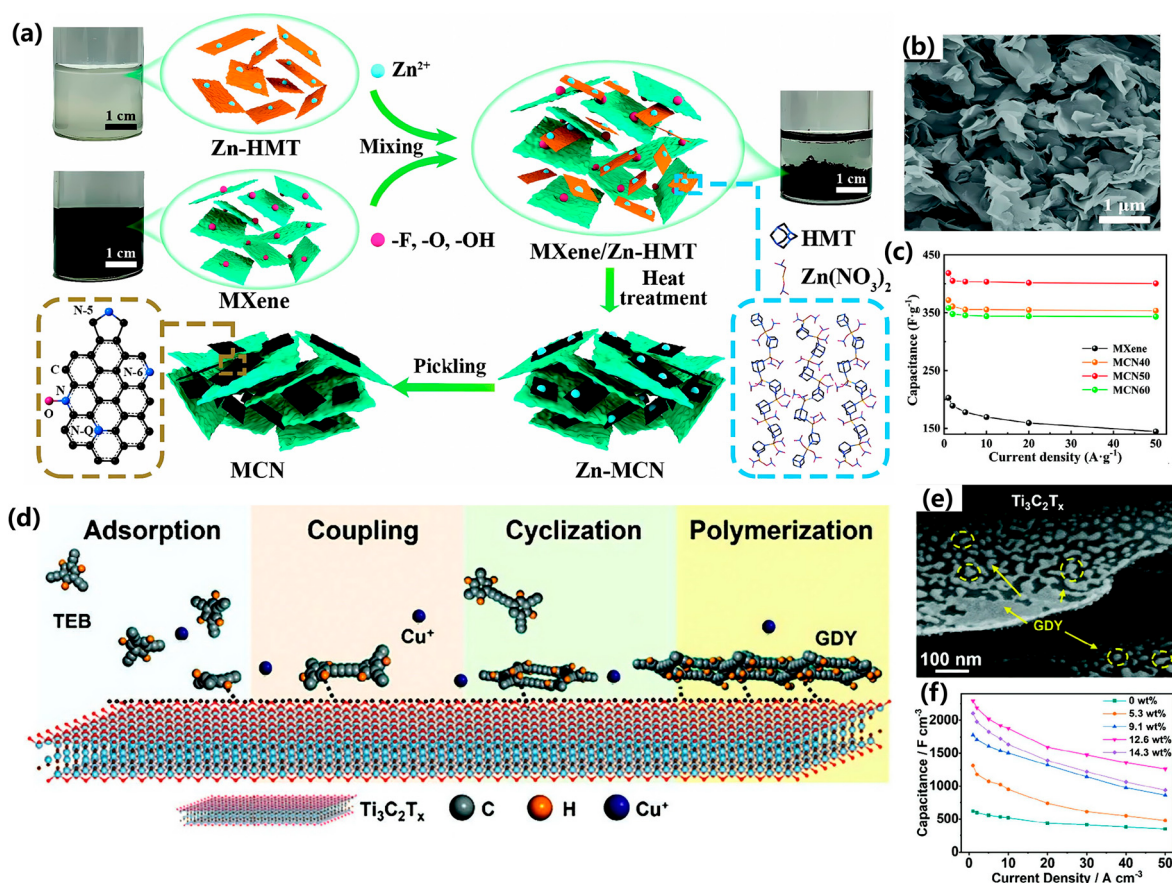


**Figure 8.** Two-dimensional carbon/MXene composites: (a) Schematic diagram and (b) SEM of MCN50, (c) capacitance value [80], copyright 2024, Wiley-VCH GmbH. (d) Schematic diagram and (e) SEM of GDY-Ti<sub>3</sub>C<sub>2</sub>T<sub>x</sub> heterostructure, (f) capacitance value [83], copyright 2024, Wiley-VCH GmbH.

Apart from a 3D structural skeleton, researchers have also studied the composite material of Ti<sub>3</sub>C<sub>2</sub>T<sub>x</sub> with carbon cloth. Li et al. reported a composite material composed of nitrogen-doped superhydrophilic carbon cloth (ENCC) and Ti<sub>3</sub>C<sub>2</sub>T<sub>x</sub> MXene nanosheets, effectively suppressing the stacking of MXene nanosheets and achieving an area-specific capacitance of  $2080.1 \text{ mF cm}^{-2}$ , as shown in Figure 10e–g [92]. Moreover, the symmetrical supercapacitor based on this composite material has a wide voltage window of 1.8V and a capacitance retention rate of 91% after 10,000 cycles. Fan et al. demonstrated a 3D porous composite material (MXene/CMDF) derived from MXene/needle punched denim felt, which achieved the removal of specific harmful groups in MXenes, exposed more active sites, and facilitated a more efficient ion exchange between electrolytes and

electrodes [93]. Therefore, the composite material exhibits a maximum specific capacitance of  $1748.5 \text{ mF cm}^{-2}$  and retained 94% capacitance after 15,000 cycles. In addition, supercapacitors based on MXene/CMDF have a specific capacitance of up to  $577.5 \text{ mF cm}^{-2}$  and a maximum energy density of  $80.2 \mu\text{Wh cm}^{-2}$ .

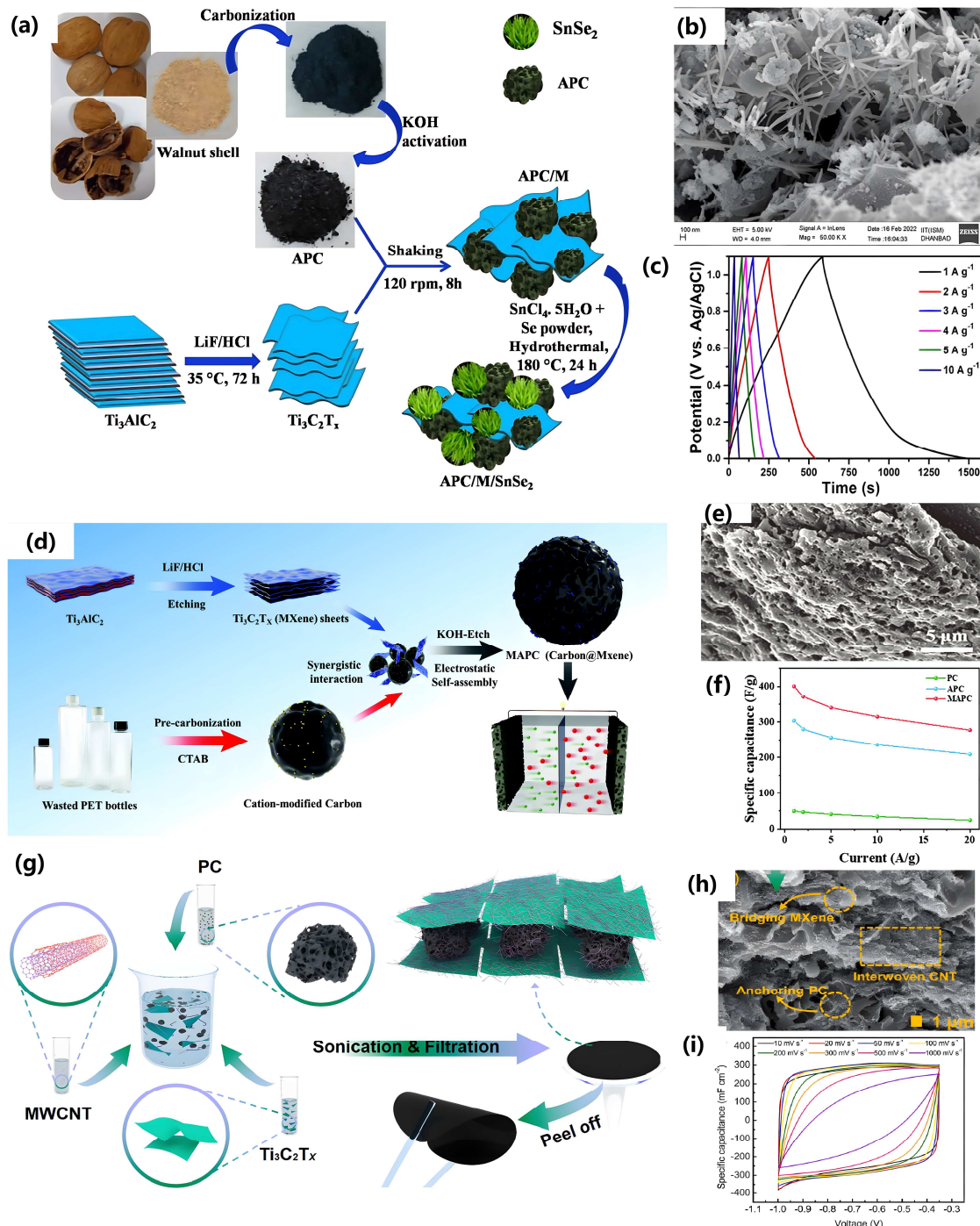


**Figure 9.** Three-dimensional carbon/MXene composites: **(a)** Schematic diagram, **(b)** SEM, and **(c)** GCD curves of APC/Ti<sub>3</sub>C<sub>2</sub>T<sub>x</sub>/SnSe<sub>2</sub> [84], copyright 2023, Elsevier. **(d)** Schematic diagram and **(e)** SEM of MAPC, **(f)** capacitance value [86], copyright 2024, Wiley-VCH GmbH. **(g)** Schematic diagram, **(h)** SEM, and **(i)** CV curves of TCP film [89], copyright 2021, Elsevier.

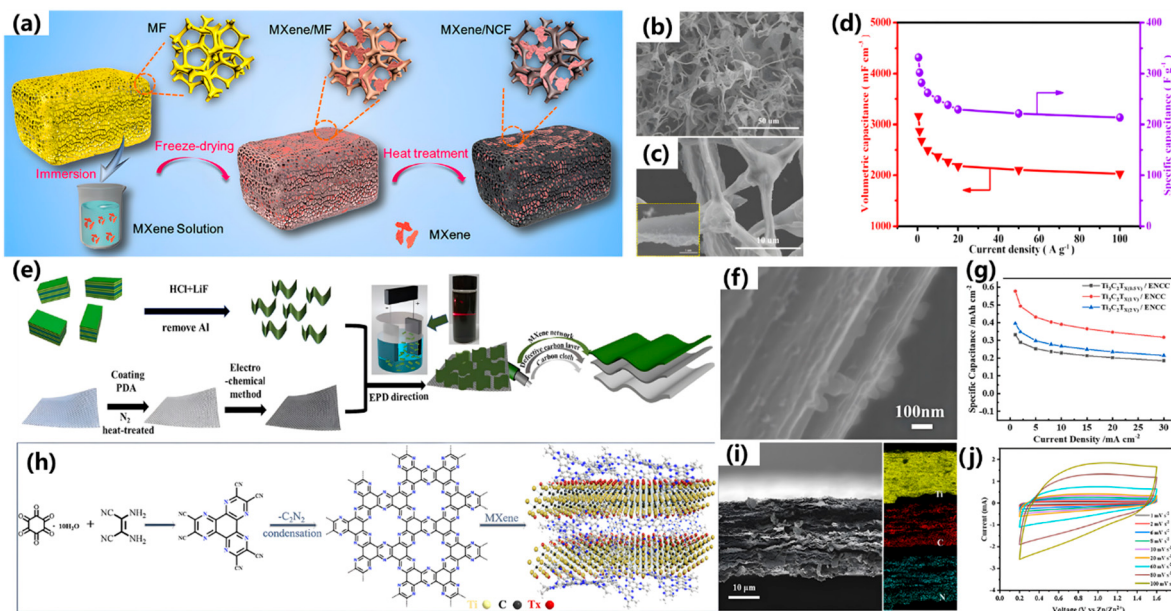


**Figure 10.** Three-dimensional carbon/MXene composites: (a) Schematic diagram, (b,c) SEM, and (d) capacitance value of MXene/NCF [91], copyright 2020, American Chemical Society. (e) Schematic diagram and (f) SEM of  $\text{Ti}_3\text{C}_2\text{T}_x/\text{ENCC}$ , (g) capacitance value [92], copyright 2022, Elsevier. Other carbon/MXenes composites: (h) Schematic diagram, (i) SEM and mapping, (j) CV curves of  $\text{C}_2\text{N}@\text{MXene}$  [94], copyright 2024, Elsevier.

### 3.5. Other Carbon/MXenes Composites

Although 0D, 1D, 2D, and 3D carbon materials combined with MXene exhibit an excellent capacitance performance, researchers have also explored the application of other carbon materials (such as  $\text{C}_2\text{N}$ , graphdiyne nanotube, CNT sponge, and so on)/MXenes composites in supercapacitors, which have demonstrated an outstanding performance. Zhao et al. designed a composite material composed of highly ordered porous nitrogen-rich carbon material  $\text{C}_2\text{N}$  and MXene nanosheets ( $\text{C}_2\text{N}@\text{MXene}$ ), as shown in Figure 10h–j [94]. The presence of MXene nanosheets enhances conductivity and suppresses the stacking phenomenon of the  $\text{C}_2\text{N}$  layer structure during repeated charge and discharge cycles, while  $\text{C}_2\text{N}$  effectively solves the self-stacking problem of MXene nanosheets. Therefore, the composite material exhibits a high specific capacitance of  $240 \text{ mAh g}^{-1}$ , a 94% capacitance retention rate after 10,000 cycles, and an energy density of  $168 \text{ Wh kg}^{-1}$ . In addition, a zinc ion micro-supercapacitor based on a  $\text{C}_2\text{N}@\text{MXene}$  electrode still exhibits a high specific capacity of  $264 \text{ mF cm}^{-2}$  and excellent flexibility characteristics. Wang et al. introduced graphene diene nanotubes (GDY NTs) with planar pores into MXene layers to construct a 3D interconnected, hydrogen-permeable MXene/Graphdiyne nanotube (MG) composite membrane [95]. The capacitance of this composite film can reach  $337.4 \text{ F g}^{-1}$  and a rate performance of 73%, which is much better than that of a pure  $\text{Ti}_3\text{C}_2\text{T}_x$  film ( $230.8 \text{ F g}^{-1}$ , 55%). Moreover, the flexible asymmetric solid-state supercapacitor based on this material exhibits a high energy density of  $19.7 \text{ Wh kg}^{-1}$  and an 88.2% capacitance retention rate after 10,000 cycles. Yang et al. reported a composite material of  $\text{Ti}_3\text{C}_2\text{T}_x$  nanosheets dispersed into an independent porous CNT sponge ( $\text{Ti}_3\text{C}_2\text{T}_x@\text{CNT}$ ) [96]. This structure provides a high-speed ion transport pathway, and MXene nanosheets can achieve pseudocapacitive contributions. Therefore, the composite material has a large capacitance value of  $468 \text{ F g}^{-1}$  and a capacitance retention of 79.8% at  $100 \text{ mV s}^{-1}$ . Huang et al. prepared a multilayer MXene superlattice with an intercalated monolayer mesoporous carbon framework (MMCF) [97]. MMCF not only increases the interlayer spacing and creates porous channels for ion transport, but also acts as a conductive pillar to guide the transfer of electrons along the z-direction. Therefore, the composite material exhibited a

volumetric capacitance of  $317 \text{ F cm}^{-3}$  and the assembled micro-supercapacitor achieved a surface energy density of  $0.10 \text{ mWh cm}^{-2}$ .

In summary, the introduction of carbon materials with different structures (0D, 1D, 2D, and 3D) into MXene has different effects on improving their electrochemical performance, as shown in Table 1 [98,99]. Zero-dimensional carbon materials have space saving encapsulation, high active sites, and a large specific surface area, effectively reducing the capacity loss caused by changes in the containment volume and the suppression of the shuttle effect [98]. One-dimensional carbon materials have the characteristic of a linear structure, which can provide a direct electron transfer path and shorten the distance of the electron transfer [19,100,101]. In addition, an excellent conductive network can be formed within the electrode, thereby prolonging electronic conduction and improving the electrochemical performance at high current densities. Two-dimensional carbon materials have a high specific surface area and excellent in-plane conductivity, increasing the in-plane electron transfer and providing sufficient active sites for electrochemical reactions. Moreover, larger lateral dimensions can be easily applied to further enhance the capacitance and rate capability of the corresponding supercapacitors [25]. Three-dimensional carbon materials with large exposed surfaces and adjustable porous structures can accelerate the electron transfer by shortening the conductive path [6]. The high surface area and porous interconnected structure can provide a large contact area with the electrolyte and a continuous ion transport path throughout the space, thereby improving the rate performance, and making it an ideal electrode material for high-performance supercapacitor applications.

**Table 1.** xD carbon/MXene composites for supercapacitors.

| Configuration   | Samples                                                                        | Specific Capacity                                       | Capacity Retention         | Ref. |
|-----------------|--------------------------------------------------------------------------------|---------------------------------------------------------|----------------------------|------|
| 0D carbon/MXene | MXene/carbon dots                                                              | $688.9 \text{ F g}^{-1}$ at $2 \text{ A g}^{-1}$        | 90% after 10,000 cycles    | [59] |
|                 | MXene/carbon dots                                                              | $1244.6 \text{ F cm}^{-3}$ at $1 \text{ A g}^{-1}$      | 93.5% after 30,000 cycles  | [60] |
|                 | Carbon spheres/MXene                                                           | $362 \text{ F g}^{-1}$ at $0.5 \text{ A g}^{-1}$        | 93.87% after 10,000 cycles | [61] |
|                 | Hollow spherical NiCo <sub>2</sub> S <sub>4</sub> /MXene/carbon                | $1786 \text{ F g}^{-1}$ at $1 \text{ A g}^{-1}$         | 100% after 10,000 cycles   | [63] |
| 1D carbon/MXene | MXene/N-CNT                                                                    | $167.2 \text{ F g}^{-1}$ at $0.5 \text{ A g}^{-1}$      | 73.2% after 10,000 cycles  | [65] |
|                 | MWCNTs-MXene@CC                                                                | $114.58 \text{ mF cm}^{-2}$ at $5 \text{ mV s}^{-1}$    | 118% after 16,000 cycles   | [66] |
|                 | MXene/CF                                                                       | $7.14 \text{ F cm}^{-3}$ at $0.5 \text{ A g}^{-1}$      | 99.8% after 5000 cycles    | [69] |
|                 | MXene/CF                                                                       | $157 \text{ F g}^{-1}$ at $5 \text{ mV s}^{-1}$         | 94% after 5000 cycles      | [70] |
| 2D carbon/MXene | MXene/CNT fiber                                                                | $295 \text{ F g}^{-1}$ at $5 \text{ mV s}^{-1}$         | 85% after 5000 cycles      | [72] |
|                 | MXene/rGO                                                                      | $274 \text{ mF cm}^{-2}$ at $1 \text{ mA cm}^{-2}$      | 96% after 100 cycles       | [75] |
|                 | Ti <sub>3</sub> C <sub>2</sub> T <sub>x</sub> /g-C <sub>3</sub> N <sub>4</sub> | $414 \text{ F g}^{-1}$ at $1 \text{ A g}^{-1}$          | 94.93% after 2500 cycles   | [78] |
|                 | MXene/carbon nanosheet                                                         | $1825.6 \text{ mF cm}^{-2}$ at $5 \text{ mA cm}^{-2}$   | 99.82% after 10,000 cycles | [79] |
| 3D carbon/MXene | GDY-Ti <sub>3</sub> C <sub>2</sub> T <sub>x</sub>                              | $2296 \text{ F cm}^{-3}$ at $1 \text{ A cm}^{-3}$       | 89.2% after 10,000 cycles  | [83] |
|                 | APC/Ti <sub>3</sub> C <sub>2</sub> T <sub>x</sub>                              | $815 \text{ F g}^{-1}$ at $1 \text{ A g}^{-1}$          | 85% after 10,000 cycles    | [84] |
|                 | MXenes/hierarchical porous carbon                                              | $404.1 \text{ F g}^{-1}$ at $1 \text{ A g}^{-1}$        | 99% after 15,000 cycles    | [86] |
|                 | N, S-MXene/3DPC                                                                | $412.7 \text{ F g}^{-1}$ at $1 \text{ A g}^{-1}$        | 97.5% after 500 cycles     | [88] |
|                 | MXene/NCF                                                                      | $332 \text{ F g}^{-1}$ at $0.5 \text{ A g}^{-1}$        | 99.2% after 10,000 cycles  | [91] |
|                 | MXene/3D needled denim felts                                                   | $1748.5 \text{ mF cm}^{-2}$ at $0.5 \text{ mA cm}^{-2}$ | 94% after 15,000 cycles    | [93] |

#### 4. Summary and Outlook

Supercapacitors, as a green, safe, and low-cost energy storage device, have received widespread attention in efficient and sustainable energy storage systems due to their unique properties, including fast charging and discharging speeds, high power density, and excellent cycle life compared to many other energy storage solutions. MXenes exhibits diversity in their elemental composition, rich surface chemistry, and atomic-level multiple configurations. Unlike other two-dimensional materials, MXenes exhibit comprehensive strength when combined with a multidimensional carbon matrix. Due to the unavoidable phenomenon of self-stacking and the aggregation of MXenes in practical applications, hybridization can be considered one of the most effective strategies. When MXenes are integrated with carbon materials, hybrid materials have potential synergistic effects, which will push the performance of MXenes-based materials to a new platform. This review

summarizes and compares various synthesis routes of carbon materials/MXenes composites and the latest research progress on the hybridization of two-dimensional MXenes with different dimensions of carbon (from 0D CQDs to 3D carbon scaffolds) to achieve an effective improvement in the electrochemical performance, namely  $x$ D carbon + 2D Mxenes =  $\infty$ . Then, based on the principle of “synthesis structure properties”, the structure property relationship of  $x$ D carbon/MXenes composite materials was systematically analyzed. However, although carbon/MXenes composites show a good performances and have made great achievements in supercapacitors’ applications, there are still many challenges and opportunities for the further development of their design and the corresponding devices, some of which are highlighted below.

Firstly, the electrochemical performance of MXenes is closely related to their surface chemistry (functional groups, atomic defects, and heteroatom doping) and microstructure (interlayer spacing and pore size). MXenes have stable synthetic properties, increased layer spacing, controllable surface functional groups, and regularized atomic defects, which are of great significance for optimizing their electrochemical performance. Further efforts to develop green, safe, economical, and scalable synthesis methods for MXenes and their composite materials, mitigate MXene oxidation, and achieve the preparation of MXenes with controllable and uniform surface ends remain a challenging task, which is crucial for advancing the industrial application of MXene-based nanostructures.

Secondly, MXenes with different chemical compositions and different properties need more exploration to build composite materials with carbon materials. More than 20 different types of MXenes have been produced in experiments. In order to improve the possibility of producing high-quality carbon/MXene electrode materials, it is necessary to conduct more in-depth and substantial research on composites constructed of different MXenes and carbon materials. Meanwhile, the performance and characteristics of each MXenes are compared to maximize the role of MXenes in the composites.

Thirdly, comprehensive research is needed to understand the fundamental mechanisms of synergistic effects between MXenes and carbon components, which will facilitate the rational design of novel composite materials with an enhanced performance and functionality. The stability design of the structure, especially the ability to withstand the volume expansion of carbon nanoparticles of different sizes during intercalation and delamination processes, is very important and worthy of attention. Therefore, in order to improve the stability of MXenes when combined with carbon, it is necessary to thoroughly study the interaction between solvents and compounds, further research and comparisons of MXene/carbon composites, and strengthen the theoretical research.

Fourth, carbon/MXene-based supercapacitors are evaluated according to actual needs. Factors such as the load density, volumetric capacity, structural stability at extremely high/low temperatures, and the safety of active materials should be considered.

Fifth, the tradeoff between mechanical properties and functions must be carefully considered. The development of high-performance, multifunctional, and digital MXenes-based supercapacitors for different application scenarios is essential without compromising their mechanical properties such as their flexibility, strength, and toughness. The development of on-chip energy storage technology for miniaturization and portable electronic devices is rapid. Micro-supercapacitors based on carbon materials/MXene have broad application prospects in future flexible and portable electronic devices due to their small size, high power density, and integration density.

Sixth, the structural evolution and reaction mechanism of MXenes-based materials need to be better understood to further design and synthesize novel MXenes and their composites with desirable properties. The clear structural evolution and charge storage mechanism will guide researchers to further improve the performance of supercapacitor devices. The advanced technology can better characterize these devices and provide unprecedented insights into mechanism elucidation.

Seventh, tailor-made synthesis techniques need to be explored to achieve precise control over the type and number of surface functional groups of Mxenes, such as a low

temperature, deoxidation, and the removal of excess salt ions, etc. The surface functional groups of MXenes have a significant impact on their electrochemical performance. However, the current synthetic approach has significant limitations. In order to synthesize MXenes with expected surface functional groups in a standardized procedure, synthesis techniques are crucial. The effective control of surface functional groups can not only improve the stability of MXenes during application, but also promote the large-scale preparation and commercial application of MXenes.

Eighth, machine learning can be used to supplement and assist experimental exploration. Machine learning is based on data-driven methods that collect data from reported research work and then train it to quickly display the best choice when weighing multiple variables.

**Funding:** This work received funding from the Shaanxi Province Qin Chuangyuan Cited High-Level Innovation and Entrepreneurship Talent Program (Approval No. QCYRCXM-2023-130) and from the Science and Technology Project of the Northwest Institute for Non-ferrous Metals Research (Approval No. 0901YK2316).

**Conflicts of Interest:** The authors declare no conflicts of interest.

## References

1. Kadam, S.A.; Kadam, K.P.; Pradhan, N.R. Advancements in 2D MXene-based supercapacitor electrodes: Synthesis, mechanisms, electronic structure engineering, flexible wearable energy storage for real-world applications, and future prospects. *J. Mater. Chem. A* **2024**, *12*, 17992–18046. [[CrossRef](#)]
2. Nidhi; Tyagi, N.; Bhardwaj, V.; Moka, S.; Singh, M.K.; Khanuja, M.; Sharma, G. An overview on synthesis of MXene and MXene based nanocomposites for supercapacitors. *Mater. Today Commun.* **2024**, *41*, 110223. [[CrossRef](#)]
3. Wang, R.; Young Jang, W.; Zhang, W.; Venkata Reddy, C.; Kakarla, R.R.; Li, C.; Gupta, V.K.; Shim, J.; Aminabhavi, T.M. Emerging two-dimensional (2D) MXene-based nanostructured materials: Synthesis strategies, properties, and applications as efficient pseudo-supercapacitors. *Chem. Eng. J.* **2023**, *472*, 144913. [[CrossRef](#)]
4. Zhou, Y.; Yin, L.; Xiang, S.; Yu, S.; Johnson, H.M.; Wang, S.; Yin, J.; Zhao, J.; Luo, Y.; Chu, P.K. Unleashing the potential of MXene-based flexible materials for high-performance energy storage devices. *Adv. Sci.* **2023**, *11*, 2304874. [[CrossRef](#)]
5. Zahra, S.A.; Anasori, B.; Iqbal, M.Z.; Ravaux, F.; Al Tarawneh, M.; Rizwan, S. Enhanced electrochemical performance of vanadium carbide MXene composites for supercapacitors. *APL Mater.* **2022**, *10*, 060901. [[CrossRef](#)]
6. Zang, X.; Wang, J.; Qin, Y.; Wang, T.; He, C.; Shao, Q.; Zhu, H.; Cao, N. Enhancing capacitance performance of  $Ti_3C_2T_x$  MXene as electrode materials of supercapacitor: From controlled preparation to composite structure construction. *Nano-Micro Lett.* **2020**, *12*, 77. [[CrossRef](#)]
7. Yu, Y.; Fan, Q.; Li, Z.; Fu, P. MXene-based electrode materials for supercapacitors: Synthesis, properties, and optimization strategies. *Mater. Today Sustain.* **2023**, *24*, 100551. [[CrossRef](#)]
8. Zhu, Y.; Ma, J.; Das, P.; Wang, S.; Wu, Z.S. High-voltage MXene-based supercapacitors: Present status and future perspectives. *Small Methods* **2023**, *7*, 2201609. [[CrossRef](#)]
9. Thomas, S.A.; Patra, A.; Al-Shehri, B.M.; Selvaraj, M.; Aravind, A.; Rout, C.S. MXene based hybrid materials for supercapacitors: Recent developments and future perspectives. *J. Energy Storage* **2022**, *55*, 105765. [[CrossRef](#)]
10. Prasankumar, T.; Manoharan, K.; Farhana, N.K.; Bashir, S.; Ramesh, K.; Ramesh, S.; Ramachandaramurthy, V.K. Advancements and approaches in developing MXene-based hybrid composites for improved supercapacitor electrodes. *Mater. Today Sustain.* **2024**, *28*, 100963. [[CrossRef](#)]
11. An, Y.; Tian, Y.; Shen, H.; Man, Q.; Xiong, S.; Feng, J. Two-dimensional MXenes for flexible energy storage devices. *Energy Environ. Sci.* **2023**, *16*, 4191–4250. [[CrossRef](#)]
12. Zan, G.; Li, S.; Chen, P.; Dong, K.; Wu, Q.; Wu, T. Mesoporous cubic nanocages assembled by coupled monolayers with 100% theoretical capacity and robust cycling. *ACS Cent. Sci.* **2024**, *10*, 1283–1294. [[CrossRef](#)] [[PubMed](#)]
13. Huang, H.; Yang, W. MXene-based micro-supercapacitors: Ink rheology, microelectrode design and integrated system. *ACS Nano* **2024**, *18*, 4651–4682. [[CrossRef](#)] [[PubMed](#)]
14. Aravind, A.M.; Tomy, M.; Kuttapan, A.; Kakkassery Aippunny, A.M.; Suryabai, X.T. Progress of 2D MXene as an electrode architecture for advanced supercapacitors: A comprehensive review. *ACS Omega* **2023**, *8*, 44375–44394. [[CrossRef](#)]
15. Chen, Y.; Yang, H.; Han, Z.; Bo, Z.; Yan, J.; Cen, K.; Ostrikov, K.K. MXene-based electrodes for supercapacitor energy storage. *Energy Fuels* **2022**, *36*, 2390–2406. [[CrossRef](#)]
16. Chen, A.; Wang, C.; Abu Ali, O.A.; Mahmoud, S.F.; Shi, Y.; Ji, Y.; Algadi, H.; El-Bahy, S.M.; Huang, M.; Guo, Z.; et al. MXene@nitrogen-doped carbon films for supercapacitor and piezoresistive sensing applications. *Compos. Part A Appl. Sci. Manuf.* **2022**, *163*, 107174. [[CrossRef](#)]

17. Siddu, N.K.P.; Jeong, S.M.; Rout, C.S. MXene-carbon based hybrid materials for supercapacitor applications. *Energy Adv.* **2024**, *3*, 341–365. [[CrossRef](#)]
18. Zhang, Y.; Feng, Z.; Wang, X.; Hu, H.; Wu, M. MXene/carbon composites for electrochemical energy storage and conversion. *Mater. Today Sustain.* **2023**, *22*, 100350. [[CrossRef](#)]
19. Cao, J.-M.; Zatovsky, I.V.; Gu, Z.-Y.; Yang, J.-L.; Zhao, X.-X.; Guo, J.-Z.; Xu, H.; Wu, X.-L. Two-dimensional MXene with multidimensional carbonaceous matrix: A platform for general-purpose functional materials. *Prog. Mater. Sci.* **2023**, *135*, 100350. [[CrossRef](#)]
20. Deng, X.; Li, J.; Ma, L.; Sha, J.; Zhao, N. Three-dimensional porous carbon materials and their composites as electrodes for electrochemical energy storage systems. *Mater. Chem. Front.* **2019**, *3*, 2221–2245. [[CrossRef](#)]
21. Ling, Z.; Ren, C.E.; Zhao, M.-Q.; Yang, J.; Giammarco, J.M.; Qiu, J.; Barsoum, M.W.; Gogotsi, Y. Flexible and conductive MXene films and nanocomposites with high capacitance. *Proc. Natl. Acad. Sci. USA* **2014**, *111*, 16676–16681. [[CrossRef](#)] [[PubMed](#)]
22. Sun, N.; Zhu, Q.; Anasori, B.; Zhang, P.; Liu, H.; Gogotsi, Y.; Xu, B. MXene-bonded flexible hard carbon film as anode for stable Na/K-ion storage. *Adv. Funct. Mater.* **2019**, *29*, 1906282. [[CrossRef](#)]
23. Cai, Y.; Chen, X.; Xu, Y.; Zhang, Y.; Liu, H.; Zhang, H.; Tang, J.  $Ti_3C_2T_x$  MXene/carbon composites for advanced supercapacitors: Synthesis, progress, and perspectives. *Carbon Energy* **2024**, *6*, e501. [[CrossRef](#)]
24. Li, L.; Cheng, Q. MXene based nanocomposite films. *Exploration* **2022**, *2*, 20220049. [[CrossRef](#)]
25. Muthukutty, B.; Kumar, P.S.; Vivekanandan, A.K.; Sivakumar, M.; Lee, S.; Lee, D. Progress and perspective in harnessing MXene-carbon-based composites (0-3D): Synthesis, performance, and applications. *Chemosphere* **2024**, *355*, e501. [[CrossRef](#)]
26. Abid, M.Z.; Rafiq, K.; Aslam, A.; Jin, R.; Hussain, E. Scope, evaluation and current perspectives of MXene synthesis strategies for state-of-the-art applications. *J. Mater. Chem. A* **2024**, *12*, 7351–7395. [[CrossRef](#)]
27. Kong, D.; Lv, W.; Liu, R.; He, Y.B.; Wu, D.; Li, F.; Fu, R.; Yang, Q.; Kang, F. Superstructured carbon materials: Design and energy applications. *Energy Mater. Devices* **2023**, *1*, 9370017. [[CrossRef](#)]
28. Hasan, M.M.; Hossain, M.M.; Chowdhury, H.K. Two-dimensional MXene-based flexible nanostructures for functional nanodevices: A review. *J. Mater. Chem. A* **2021**, *9*, 3231–3269. [[CrossRef](#)]
29. Gao, M.; Wang, F.; Yang, S.; Gaetano Ricciardulli, A.; Yu, F.; Li, J.; Sun, J.; Wang, R.; Huang, Y.; Zhang, P.; et al. Engineered 2D MXene-based materials for advanced supercapacitors and micro-supercapacitors. *Mater. Today* **2024**, *72*, 318–358. [[CrossRef](#)]
30. Wang, C.; Chen, S.; Song, L. Tuning 2D MXenes by surface controlling and interlayer engineering: Methods, properties, and synchrotron radiation characterizations. *Adv. Funct. Mater.* **2020**, *30*, 2000869. [[CrossRef](#)]
31. Bi, W.; Gao, G.; Li, C.; Wu, G.; Cao, G. Synthesis, properties, and applications of MXenes and their composites for electrical energy storage. *Prog. Mater. Sci.* **2024**, *142*, 101227. [[CrossRef](#)]
32. Kshetri, T.; Tran, D.T.; Le, H.T.; Nguyen, D.C.; Hoa, H.V.; Kim, N.H.; Lee, J.H. Recent advances in MXene-based nanocomposites for electrochemical energy storage applications. *Prog. Mater. Sci.* **2021**, *117*, 100733. [[CrossRef](#)]
33. Chetana, S.; Mohd Abdah, M.A.A.; Thakur, V.N.; Govinde Gowda, M.S.; Choudhary, P.; Sriramoju, J.B.; Rangappa, D.; Malik, S.; Rustagi, S.; Khalid, M. Progress and prospects of MXene-based hybrid composites for next-generation energy technology. *J. Electrochem. Soc.* **2023**, *170*, 120530. [[CrossRef](#)]
34. Yang, G.; Liu, D.; Lei, W. MXene-based nanocomposites for nanofluidic energy conversion: A review. *Adv. Nanocompos.* **2024**, *1*, 94–109. [[CrossRef](#)]
35. Deng, Q.; Liu, F.Z.; Wu, X.W.; Li, C.Z.; Zhou, W.B.; Long, B. An aqueous  $BiI_3$ -Zn battery with dual mechanisms of  $Zn^{2+}$  (de)intercalation and  $I^-/I_2$  redox. *J. Energy Chem.* **2024**, *89*, 670–678. [[CrossRef](#)]
36. Sagadevan, S.; Fatimah, I.; Lett, J.A.; Kakavandi, B.; Soga, T.; Oh, W.-C.; Randriamahazaka, H. Exploring the potential of MXene-based aerogels and hybrid nanocomposites for supercapacitor applications. *J. Energy Storage* **2024**, *99*, 113269. [[CrossRef](#)]
37. Jiang, S.; Lu, L.; Song, Y. Recent advances of flexible MXene and its composites for supercapacitors. *Chem.-Eur. J.* **2024**, *30*, e202304036. [[CrossRef](#)] [[PubMed](#)]
38. Liu, Y.; Yu, J.; Guo, D.; Li, Z.; Su, Y.  $Ti_3C_2T_x$  MXene/graphene nanocomposites: Synthesis and application in electrochemical energy storage. *J. Alloys Compd.* **2020**, *815*, 152403. [[CrossRef](#)]
39. Qi, M.; Li, F.; Zhang, Z.; Lai, Q.; Liu, Y.; Gu, J.; Wang, L. Three-dimensional interconnected ultrathin manganese dioxide nanosheets grown on carbon cloth combined with  $Ti_3C_2T_x$  MXene for high-capacity zinc-ion batteries. *J. Colloid Interface Sci.* **2022**, *615*, 151–162. [[CrossRef](#)]
40. Shi, X.; Liang, W.; Liu, G.; Chen, B.; Shao, L.; Wu, Y.; Sun, Z.; García, F. Electrode materials for Li/Na storage from mechanochemically synthesised MOFs/MXene Composites: A Solvent-free approach. *Chem. Eng. J.* **2023**, *462*, 142271. [[CrossRef](#)]
41. Fu, X.-Y.; Shu, R.-Y.; Ma, C.-J.; Zhang, Y.-Y.; Jiang, H.-B. Laser-induced fabrication of electrodes on graphene oxide-MXene composites for planar supercapacitors. *ACS Appl. Nano Mater.* **2023**, *6*, 4567–4572. [[CrossRef](#)]
42. Depijan, M.; Hantanasirisakul, K.; Pakawatpanurut, P. Interfacial engineering of  $Ti_3C_2T_x$  MXene electrode using g-C<sub>3</sub>N<sub>4</sub> nanosheets for high-performance supercapacitor in neutral electrolyte. *ACS Omega* **2024**, *9*, 22256–22264. [[CrossRef](#)] [[PubMed](#)]
43. Hong, Z.; Tian, H.; Fang, Z.; Wu, H.; Zhao, F.; Li, Q.; Fan, S.; Wang, J.; Liu, P. Carbon nanotube/MXene composite with a dense regular connective tissue structure and its application in lithium-ion batteries. *ACS Appl. Energy Mater.* **2024**, *7*, 8004–8013. [[CrossRef](#)]
44. Yu, L.; Hu, L.; Anasori, B.; Liu, Y.-T.; Zhu, Q.; Zhang, P.; Gogotsi, Y.; Xu, B. MXene-bonded activated carbon as a flexible electrode for high-performance supercapacitors. *ACS Energy Lett.* **2018**, *3*, 1597–1603. [[CrossRef](#)]

45. Wang, G.; Li, C.; Estevez, D.; Xu, P.; Peng, M.; Wei, H.; Qin, F. Boosting interfacial polarization through heterointerface engineering in MXene/graphene intercalated-based microspheres for electromagnetic wave absorption. *Nano-Micro Lett.* **2023**, *15*, 152. [[CrossRef](#)]
46. Lei, J.; Yu, F.; Xie, H.; Ma, J.  $Ti_3C_2T_x$  MXene/carbon nanofiber multifunctional electrode for electrode ionization with antifouling activity. *Chem. Sci.* **2023**, *14*, 3610–3621. [[CrossRef](#)]
47. Wang, Z.; Huang, Z.; Wang, H.; Li, W.; Wang, B.; Xu, J.; Xu, T.; Zang, J.; Kong, D.; Li, X.; et al. 3D-printed sodiophilic  $V_2CT_x/rGO-CNT$  MXene microgrid aerogel for stable Na metal anode with high areal capacity. *ACS Nano* **2022**, *16*, 9105–9116. [[CrossRef](#)]
48. Dai, Y.; Wu, X.; Li, L.; Zhang, Y.; Deng, Z.; Yu, Z.-Z.; Zhang, H.-B. 3D printing of resilient, lightweight and conductive MXene/reduced graphene oxide architectures for broadband electromagnetic interference shielding. *J. Mater. Chem. A* **2022**, *10*, 11375–11385. [[CrossRef](#)]
49. Zhu, W.; Zhuang, Y.; Weng, J.; Huang, Q.; Lai, G.; Li, L.; Chen, M.; Xia, K.; Lu, Z.; Wu, M.; et al. Evolution of naturally dried MXene-based composite aerogels with flash joule annealing for large-scale production of highly sensitive customized sensors. *Adv. Mater.* **2024**, *36*, 2407138. [[CrossRef](#)]
50. Sangili, A.; Unnikrishnan, B.; Nain, A.; Hsu, Y.-J.; Wu, R.-S.; Huang, C.-C.; Chang, H.-T. Stable carbon encapsulated titanium carbide MXene aqueous ink for fabricating high-performance supercapacitors. *Energy Storage Mater.* **2022**, *53*, 51–61. [[CrossRef](#)]
51. Allah, A.E.; Wang, J.; Kaneti, Y.V.; Li, T.; Farghali, A.A.; Khedr, M.H.; Nanjundan, A.K.; Ding, B.; Dou, H.; Zhang, X.; et al. Auto-programmed heteroarchitecturing: Self-assembling ordered mesoporous carbon between two-dimensional  $Ti_3C_2T_x$  MXene layers. *Nano Energy* **2019**, *65*, 103991. [[CrossRef](#)]
52. Zhang, Y.; Lan, D.; Hou, T.; Jia, M.; Jia, Z.; Gu, J.; Wu, G. Multifunctional electromagnetic wave absorbing carbon fiber/ $Ti_3C_2T_x$  MXene fabric with ultra-wide absorption band. *Carbon* **2024**, *230*, 119594. [[CrossRef](#)]
53. Ma, C.; Ma, M.G.; Si, C.; Ji, X.X.; Wan, P. Flexible MXene-based composites for wearable devices. *Adv. Funct. Mater.* **2021**, *31*, 2009524. [[CrossRef](#)]
54. Sun, M.; Ye, W.; Zhang, J.; Zheng, K. Structure, properties, and preparation of MXene and the application of its composites in supercapacitors. *Inorganics* **2024**, *12*, 112. [[CrossRef](#)]
55. Vijayakumar, M.; Elsa, G.; Nirogi, A.; Navaneethan, R.; Sankar, A.B.; Karthik, M. MXenes and their composites for hybrid capacitors and supercapacitors: A critical review. *Emergent Mater.* **2021**, *4*, 655–672. [[CrossRef](#)]
56. Forouzandeh, P.; Pillai, S.C. MXenes-based nanocomposites for supercapacitor applications. *Curr. Opin. Chem. Eng.* **2021**, *33*, 100710. [[CrossRef](#)]
57. Das, P.; Ganguly, S.; Rosenkranz, A.; Wang, B.; Yu, J.; Srinivasan, S.; Rajabzadeh, A.R. MXene/0D nanocomposite architectures: Design, properties and emerging applications. *Mater. Today Nano* **2023**, *24*, 100428. [[CrossRef](#)]
58. Elemike, E.E.; Adeyemi, J.; Onwudiwe, D.C.; Wei, L.; Oyedeleji, A.O. The future of energy materials: A case of MXenes-carbon dots nanocomposites. *J. Energy Storage* **2022**, *50*, 104711. [[CrossRef](#)]
59. Wang, Y.; Chen, N.; Zhou, B.; Zhou, X.; Pu, B.; Bai, J.; Tang, Q.; Liu, Y.; Yang, W.  $NH_3$ -induced in situ etching strategy derived 3D-interconnected porous MXene/carbon dots films for high performance flexible supercapacitors. *Nano-Micro Lett.* **2023**, *15*, 231. [[CrossRef](#)]
60. Zhang, P.; Li, J.; Yang, D.; Soomro, R.A.; Xu, B. Flexible carbon dots-intercalated MXene film electrode with outstanding volumetric performance for supercapacitors. *Adv. Funct. Mater.* **2022**, *33*, 2209918. [[CrossRef](#)]
61. Wei, L.; Deng, W.; Li, S.; Wu, Z.; Cai, J.; Luo, J. Sandwich-like chitosan porous carbon Spheres/MXene composite with high specific capacitance and rate performance for supercapacitors. *J. Bioresour. Bioprod.* **2022**, *7*, 63–72. [[CrossRef](#)]
62. Yang, F.; Lv, K.; Zhao, X.; Kong, D.; Kong, N.; Luo, Z.; Tao, J.; Zhou, J.; Razal, J.M.; Zhang, J. Hierarchical heterostructures of MXene and mesoporous hollow carbon sphere for improved ion accessibility and rate performance. *Chem. Eng. J.* **2024**, *494*, 153426. [[CrossRef](#)]
63. Li, B.; Zhang, L.; Zhao, Z.; Zou, Y.; Chen, B.; Fu, X.; Wang, F.; Long, S.; Guo, W.; Liang, J.; et al. Unraveling hierarchical hollow  $NiCo_2S_4$ /MXene/N-doped carbon microspheres via dual templates for high-performance hybrid supercapacitors. *Chem. Eng. J.* **2024**, *487*, 150730. [[CrossRef](#)]
64. Mohajer, F.; Ziarani, G.M.; Badiei, A.; Iravani, S.; Varma, R.S. MXene-carbon nanotube composites: Properties and applications. *Nanomaterials* **2023**, *13*, 345. [[CrossRef](#)]
65. Wang, Q.; Yuan, H.; Zhang, M.; Yang, N.; Cong, S.; Zhao, H.; Wang, X.; Xiong, S.; Li, K.; Zhou, A. A highly conductive and supercapacitive MXene/N-CNT electrode material derived from a MXene-Co-melamine precursor. *ACS Appl. Electron. Mater.* **2023**, *5*, 2506–2517. [[CrossRef](#)]
66. Li, H.; Chen, R.; Ali, M.; Lee, H.; Ko, M.J. In situ grown MWCNTs/MXenes nanocomposites on carbon cloth for high-performance flexible supercapacitors. *Adv. Funct. Mater.* **2020**, *30*, 2002739. [[CrossRef](#)]
67. Hakim, M.W.; Ali, I.; Fatima, S.; Li, H.; Jafri, S.H.M.; Rizwan, S. Enhanced electrochemical performance of MWCNT-assisted molybdenum-titanium carbide MXene as a potential electrode material for energy storage application. *ACS Omega* **2024**, *9*, 8763–8772. [[CrossRef](#)]
68. You, M.; Xin, B. MXene nanosheets and carbon nanofiber hybrid membranes for electrochemical energy storage materials. *Fibers Polym.* **2024**, *25*, 3323–3330. [[CrossRef](#)]

69. Sun, L.; Fu, Q.; Pan, C. Hierarchical porous “skin/skeleton”-like MXene/biomass derived carbon fibers heterostructure for self-supporting, flexible all solid-state supercapacitors. *J. Hazard. Mater.* **2021**, *410*, 124565. [[CrossRef](#)]
70. Dharmasiri, B.; Usman, K.A.S.; Qin, S.A.; Razal, J.M.; Tran, N.T.; Coia, P.; Harte, T.; Henderson, L.C.  $Ti_3C_2T_x$  MXene coated carbon fibre electrodes for high performance structural supercapacitors. *Chem. Eng. J.* **2023**, *476*, 146739. [[CrossRef](#)]
71. Song, W.; Wang, K.; Lian, X.; Zheng, F.; Niu, H. Non-preoxidation synthesis of MXene integrated flexible carbon film for supercapacitors. *Chem. Eng. J.* **2024**, *493*, 152804. [[CrossRef](#)]
72. Zhao, X.; Zhang, J.; Lv, K.; Kong, N.; Shao, Y.; Tao, J. Carbon nanotubes boosts the toughness and conductivity of wet-spun MXene fibers for fiber-shaped super capacitors. *Carbon* **2022**, *200*, 38–46. [[CrossRef](#)]
73. Zarepour, A.; Ahmadi, S.; Rabiee, N.; Zarrabi, A.; Iravani, S. Self-healing MXene- and graphene-based composites: Properties and applications. *Nano-Micro Lett.* **2023**, *15*, 100. [[CrossRef](#)]
74. Dang, A.; Han, Y.; Sun, Y.; Liu, Y.; Zhao, Z.; Liu, X.; Zada, A.; Han, Y.; Li, T.; Li, J. Mechanically stable reduced graphene oxide/MXene fibers with exceptional volumetric capacitance and energy density mediated by carbon nanotubes for high-performance symmetrical supercapacitors. *ACS Appl. Energy Mater.* **2024**, *7*, 5548–5558. [[CrossRef](#)]
75. Qin, Z.; Wang, Z.; Li, D.; Lv, Y.; Zhao, B.; Pan, K. Nanofiber-reinforced MXene/rGO composite aerogel for a high-performance piezoresistive sensor and an all-solid-state supercapacitor electrode material. *ACS Appl. Mater. Interfaces* **2024**, *16*, 32554–32565. [[CrossRef](#)] [[PubMed](#)]
76. Li, Y.; Xu, L.; Dai, J.; Zhu, H.-X.; Wang, S.-J. Multidimensional nanostructural engineering of MXene-based composite films for high-performance supercapacitors. *Energy Fuels* **2024**, *38*, 5493–5505. [[CrossRef](#)]
77. Xu, C.; Tong, L.; Zhang, W.; Zhao, X.; Yang, L.; Yin, S. One-step synthesis of  $g\text{-}C_3N_4/TiVCT_x$  MXene electrodes for lithium-ion batteries and supercapacitors. *Chem. Eng. J.* **2024**, *497*, 154449. [[CrossRef](#)]
78. Zhang, S.; Huang, Y.; Wang, J.; Han, X.; Chen, C.; Sun, X.  $Ti_3C_2T_x/g\text{-}C_3N_4$  heterostructure films with outstanding capacitance for flexible Solid-state supercapacitors. *Appl. Surf. Sci.* **2022**, *599*, 154015. [[CrossRef](#)]
79. Zhang, S.; Huang, Y.; Ruan, Y.; Wang, J.; Han, X.; Sun, X. Electrostatic self-assembly of citrus based carbon nanosheets and MXene: Flexible film electrodes and patterned interdigital electrodes for all-solid supercapacitors. *J. Energy Storage* **2023**, *58*, 106392. [[CrossRef](#)]
80. Chen, A.; Wei, H.; Peng, Z.; Wang, Y.; Akinlabi, S.; Guo, Z.; Gao, F.; Duan, S.; He, X.; Jia, C.; et al. MXene/nitrogen-doped carbon nanosheet scaffold electrode toward high-performance solid-state zinc ion supercapacitor. *Small* **2024**, *20*, 2404011. [[CrossRef](#)]
81. Mo, T.; Wang, Z.; Zeng, L.; Chen, M.; Kornyshev, A.A.; Zhang, M.; Zhao, Y.; Feng, G. Energy storage mechanism in supercapacitors with porous graphdiynes: Effects of pore topology and electrode metallicity. *Adv. Mater.* **2023**, *35*, 2301118. [[CrossRef](#)] [[PubMed](#)]
82. Zheng, X.; Chen, S.; Li, J.; Wu, H.; Zhang, C.; Zhang, D.; Chen, X.; Gao, Y.; He, F.; Hui, L.; et al. Two-dimensional carbon graphdiyne: Advances in fundamental and application research. *ACS Nano* **2023**, *17*, 14309–14346. [[CrossRef](#)] [[PubMed](#)]
83. Wu, D.; Zhang, Y.; Man, Z.; Zhang, H.; Zhu, X.; Ding, J.; Xu, J.; Bao, N.; Lu, W. In situ fabrication of graphdiyne nanoisland anchored  $Ti_3C_2T_x$  film to accelerate intercalation pseudocapacitance kinetics. *Adv. Energy Mater.* **2024**, *14*, 2304404. [[CrossRef](#)]
84. De, S.; Maity, C.K.; Kim, M.J.; Nayak, G.C. Tin(IV) selenide anchored-biowaste derived porous carbon- $Ti_3C_2T_x$  (MXene) nanohybrid: An ionic electrolyte enhanced high performing flexible supercapacitor electrode. *Electrochim. Acta* **2023**, *463*, 142811. [[CrossRef](#)]
85. Yong, S.; Yao, C.; Hillier, N.; Kim, H.; Holicky, M.; Liu, S.; Doherty, R.; Torrisi, F.; Beeby, S.  $Ti_3C_2$  MXene as additive for low-cost textile supercapacitors with enhanced electrical performance. *Adv. Mater. Technol.* **2023**, *9*, 2301266. [[CrossRef](#)]
86. Hou, X.; Ren, P.; Tian, W.; Xue, R.; Tong, W.; Chen, Z.; Ren, F.; Jin, Y. Electrostatic self-assembly heterostructured MXenes/wasted PET-derived carbon for superior capacitive energy storage. *Adv. Mater. Technol.* **2024**, *9*, 2301766. [[CrossRef](#)]
87. Seenath, J.S.; Biswal, B.P. Construction of MXene-coupled nitrogen-doped porous carbon hybrid from a conjugated microporous polymer for high-performance supercapacitors. *Adv. Energy Sustain. Res.* **2021**, *2*, 2000052. [[CrossRef](#)]
88. Huang, Y.; Xu, Y.; Wang, J.; Bao, S.; Zhang, Y.; Yin, Y.; Lu, J. Self-assembly of N,S-MXene/3DPC heterostructure with multiple charge transfer channels for high-performance supercapacitors and sodium-ion batteries. *J. Power Sources* **2024**, *601*, 234312. [[CrossRef](#)]
89. Yang, K.; Luo, M.; Zhang, D.; Liu, C.; Li, Z.; Wang, L.; Chen, W.; Zhou, X.  $Ti_3C_2T_x$ /carbon nanotube/porous carbon film for flexible supercapacitor. *Chem. Eng. J.* **2022**, *427*, 132002. [[CrossRef](#)]
90. Yao, W.; Zheng, D.; Li, Z.; Wang, Y.; Tan, H.; Zhang, Y. MXene@ carbonized wood monolithic electrode with hierarchical porous framework for high-performance supercapacitors. *Appl. Surf. Sci.* **2023**, *638*, 158130. [[CrossRef](#)]
91. Sun, L.; Song, G.; Sun, Y.; Fu, Q.; Pan, C. MXene/N-doped carbon foam with three-dimensional hollow neuron-like architecture for freestanding, highly compressible all solid-state supercapacitors. *ACS Appl. Mater. Interfaces* **2020**, *12*, 44777–44788. [[CrossRef](#)] [[PubMed](#)]
92. Li, Z.; Liu, X.; Wang, X.; Wang, H.; Ren, J.; Wang, R. Electrophoretic deposition of  $Ti_3C_2T_x$  MXene nanosheet N-carbon cloth as binder-free supercapacitor electrode material. *J. Alloys Compd.* **2022**, *927*, 166934. [[CrossRef](#)]
93. Fan, W.; Wang, Q.; Rong, K.; Shi, Y.; Peng, W.; Li, H.; Guo, Z.; Xu, B.B.; Hou, H.; Algadi, H.; et al. MXene enhanced 3D needled waste denim felt for high-performance flexible supercapacitors. *Nano-Micro Lett.* **2023**, *16*, 36. [[CrossRef](#)] [[PubMed](#)]
94. Zhao, D.; Xu, D.; Wang, T.; Yang, Z. Nitrogen-rich nanoporous carbon with MXene composite for high-performance Zn-ion hybrid capacitors. *Mater. Today Energy* **2024**, *45*, 101671. [[CrossRef](#)]

95. Wang, Y.; Chen, N.; Liu, Y.; Zhou, X.; Pu, B.; Qing, Y.; Zhang, M.; Jiang, X.; Huang, J.; Tang, Q.; et al. MXene/graphdiyne nanotube composite films for free-standing and flexible solid-state supercapacitor. *Chem. Eng. J.* **2022**, *450*, 138398. [[CrossRef](#)]
96. Yang, R.; Hu, Q.; Yang, S.; Zeng, Z.; Zhang, H.; Cao, A.; Gui, X. Anchoring oxidized MXene nanosheets on porous carbon nanotube sponge for enhancing ion transport and pseudocapacitive performance. *ACS Appl. Mater. Interfaces* **2022**, *14*, 41997–42006. [[CrossRef](#)]
97. Huang, X.; Lyu, X.; Wu, G.; Yang, J.; Zhu, R.; Tang, Y.; Li, T.; Wang, Y.; Yang, D.; Dong, A. Multilayer superlattices of monolayer mesoporous carbon framework-intercalated MXene for efficient capacitive energy storage. *Adv. Energy Mater.* **2023**, *14*, 2303417. [[CrossRef](#)]
98. Zhao, Y.; Zhang, Y.; Wang, Y.; Cao, D.; Sun, X.; Zhu, H. Versatile zero- to three-dimensional carbon for electrochemical energy storage. *Carbon Energy* **2021**, *3*, 895–915. [[CrossRef](#)]
99. Cai, Z.; Ma, Y.F.; Wang, M.; Qian, A.N.; Tong, Z.M.; Xiao, L.T.; Jia, S.T.; Chen, X.Y. Engineering of electrolyte ion channels in MXene/holey graphene electrodes for superior supercapacitive performances. *Rare Met.* **2022**, *41*, 2084–2093. [[CrossRef](#)]
100. Long, B.; Liang, X.; Pei, Y.; Wu, X.; Wang, X.; Law, M.K. Free-standing bioi@mwcnts photoelectrodes for photo-rechargeable zinc-ion batteries. *J. Mater. Sci. Technol.* **2024**, *198*, 137–142. [[CrossRef](#)]
101. Long, B.; Ma, X.Y.; Chen, L.J.; Song, T.; Pei, Y.; Wang, X.Y.; Wu, X.W. Se Vacancy Activated Bi<sub>2</sub>Se<sub>3</sub> Nanodots Encapsulated in Porous Carbon Nanofibers for Aqueous Zinc and Ammonium Ion Batteries. In *Advanced Functional Materials*; Wiley Online Library: Hoboken, NJ, USA, 2024; p. 2411430. [[CrossRef](#)]

**Disclaimer/Publisher's Note:** The statements, opinions and data contained in all publications are solely those of the individual author(s) and contributor(s) and not of MDPI and/or the editor(s). MDPI and/or the editor(s) disclaim responsibility for any injury to people or property resulting from any ideas, methods, instructions or products referred to in the content.